GEOSPHERE

GEOSPHERE, v. 17

https://doi.org/10.1130/GES02319.1

12 figures; 2 tables; 1 set of supplemental files

CORRESPONDENCE: matt.heizler@nmt.edu

CITATION: Heizler, M.T., Karlstrom, K.E., Albonico, M., Hereford, R., Beard, L.S., Cather, S.M., Crossey, L.J., and Sundell, K.E., 2021, Detrital sanidine $^{40}Ar/^{39}Ar$ dating confirms <2 Ma age of Crooked Ridge paleoriver and subsequent deep denudation of the southwestern Colorado Plateau: Geosphere, v. 17, https://doi.org/10.1130/GES02319.1.

Science Editor: Andrea Hampel
Associate Editor: Christopher J. Spencer

Received 15 July 2020
Revision received 11 September 2020
Accepted 15 January 2021

Detrital sanidine $^{40}Ar/^{39}Ar$ dating confirms <2 Ma age of Crooked Ridge paleoriver and subsequent deep denudation of the southwestern Colorado Plateau

Matthew T. Heizler[1], Karl E. Karlstrom[2], Micael Albonico[2], Richard Hereford[3], L. Sue Beard[3], Steven M. Cather[1], Laurie J. Crossey[2], and Kurt E. Sundell[4]

[1]New Mexico Bureau of Geology and Mineral Resources, New Mexico Tech, 801 Leroy Place, Socorro, New Mexico 87801, USA
[2]University of New Mexico, 221 Yale Boulevard NE, Albuquerque, New Mexico 87106, USA
[3]U.S. Geological Survey, 2255 N. Gemini Drive, Flagstaff, Arizona 86001, USA
[4]University of Arizona, 1040 E. 4th Street, Tucson, Arizona 85721, USA

ABSTRACT

Crooked Ridge and White Mesa in northeastern Arizona (southwestern United States) preserve, as inverted topography, a 57-km-long abandoned alluvial system near the present drainage divide between the Colorado, San Juan, and Little Colorado Rivers. The pathway of this paleoriver, flowing southwest toward eastern Grand Canyon, has led to provocative alternative models for its potential importance in carving Grand Canyon. The ~50-m-thick White Mesa alluvium is the only datable record of this paleoriver system. We present new $^{40}Ar/^{39}Ar$ sanidine dating that confirms a ca. 2 Ma maximum depositional age for White Mesa alluvium, supported by a large mode (n = 42) of dates from 2.06 to 1.76 Ma. Older grain modes show abundant 37–23 Ma grains mostly derived ultimately from the San Juan Mountains, as is also documented by rare volcanic and basement pebbles in the White Mesa alluvium. A tuff with an age of 1.07 ± 0.05 Ma is inset below, and hence provides a younger age bracket for the White Mesa alluvium. Newly dated remnant deposits on Black Mesa contain similar 37–23 Ma grains and exotic pebbles, plus a large mode (n = 71) of 9.052 ± 0.003 Ma sanidine. These deposits could be part of the White Mesa alluvium without any Pleistocene grains, but new detrital sanidine data from the upper Bidahochi Formation near Ganado, Arizona, have similar maximum depositional ages of 11.0–6.1 Ma and show similar 40–20 Ma San Juan Mountains–derived sanidine. Thus, we tentatively interpret the <9 Ma Black Mesa deposit to be a remnant of an 11–6 Ma Bidahochi alluvial system derived from the now-eroded southwestern fringe of the San Juan Mountains. This alluvial fringe is the probable source for reworking of 40–20 Ma detrital sanidine and exotic clasts into Oligocene Chuska Sandstone, Miocene Bidahochi Formation, and ultimately into the <2 Ma White Mesa alluvium. The <2 Ma age of the White Mesa alluvium does not support models that the Crooked Ridge paleoriver originated as a late Oligocene to Miocene San Juan River that ultimately carved across the Kaibab uplift. Instead, we interpret the Crooked Ridge paleoriver as a 1.9–1.1 Ma tributary to the Little Colorado River, analogous to modern-day Moenkopi Wash. We reject the "young sediment in old paleovalley" hypothesis based on mapping, stratigraphic, and geomorphic constraints. Deep exhumation and beheading by tributaries of the San Juan and Colorado Rivers caused the Crooked Ridge paleotributary to be abandoned between 1.9 and 1.1 Ma. Thermochronologic data also provide no evidence for, and pose substantial difficulties with, the hypothesis for an earlier (Oligocene–Miocene) Colorado–San Juan paleoriver system that flowed along the Crooked Ridge pathway and carved across the Kaibab uplift.

Matthew Heizler https://orcid.org/0000-0002-3911-4932

INTRODUCTION

Reconstructing the age and evolution of paleolandscapes in the Colorado Plateau–Grand Canyon region (southwestern United States) continues to provide stimulating debate that can foster development of improved dating and landscape models. For decades, geologists have speculated about possible evolution of paleoriver pathways and have debated "old" (ca. 70 Ma), "intermediate" (ca. 25 Ma), and "young" (post–10 Ma) models to explain the modern iconic landscape of the Grand Canyon region (e.g., Karlstrom et al., 2012a). Preserved paleoriver deposits are relatively scarce due to deep erosion of the Colorado Plateau region, yet these remnants provide some of the most important data sets for reconstructing landscape evolution to the extent their ages and pathways are known.

Gravels of Crooked Ridge and White Mesa area (northeastern Arizona) have been part of models for the evolution of the Colorado River system and carving of Grand Canyon for many decades. Various workers have envisioned that an Oligocene–early Miocene river flowed southwest from Utah into Arizona along the Crooked Ridge pathway (Babenroth and Strahler, 1945; Strahler, 1948; Cooley and Davidson, 1963; McKee et al., 1967; Hunt, 1969; Lucchitta et al., 2011, 2013). The models differ regarding how and when such a Colorado–San Juan paleoriver got integrated across the Kaibab uplift to carve Grand Canyon. The alignment of the Crooked Ridge deposits with a 2.5-km-wide break in the Echo Cliffs called

"The Gap" and with the segment of eastern Grand Canyon that cuts across the Kaibab uplift (Fig. 1) make the Crooked Ridge deposits a potential candidate for the remains of a major paleoriver.

The deposits were mapped by Cooley and Davidson (1963, their figure 10) as the "gravel on White Mesa" and interpreted as a late Miocene and Pliocene ancestral Colorado River–San Juan River system. Cooley et al. (1969, their plate 1) showed the name "Crooked Ridge" for a ridge of the outcropping gravels. Hunt (1969, his figures 68, 69) called these sediments the "Tertiary gravel of Kaibito Plateau" and also interpreted them to have been deposited by a pre–late Miocene San Juan paleoriver. All of these workers considered the deposits on White Mesa and Crooked Ridge to be the same map unit.

Lucchitta et al. (2011, 2013) reinvigorated discussion of these deposits and named the "Crooked Ridge River". We choose the term "Crooked Ridge paleoriver" because there is no current Crooked Ridge [sic]. They characterized the pebble and cobble types in the alluvium and made the argument (as did Hunt [1969] p. 106) that "exotic" clasts of volcanic and basement lithologies came from the San Juan Mountains located to the northeast, and that these are deposits of a major river, the San Juan paleoriver.

Hereford et al. (2016) mapped and characterized the 50-m-thick succession of gravel, sand, and silt and called it the White Mesa alluvium. They reported four <2 Ma detrital sanidine grains in the White Mesa alluvium, an unexpectedly young age. By applying the surface mapping of Cooley et al. (1969) with other known incision rates and ash dates on surfaces of different landscape position, these authors proposed that the White Mesa alluvium is <2 Ma and was deposited by a former tributary to the Little Colorado River rather than a major trunk river. Karlstrom et al. (2017) suggested that its landscape position records a denudation history for the region consistent with rapid incision

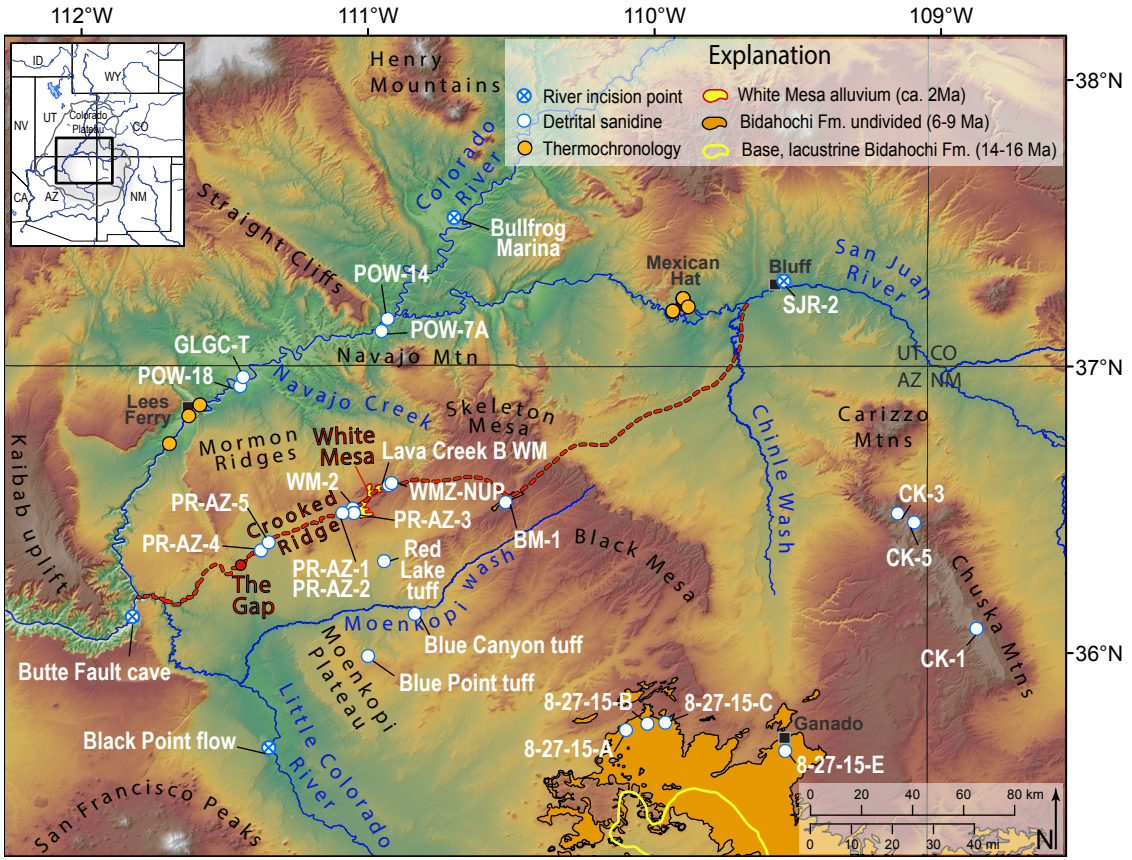

Figure 1. Crooked Ridge paleoriver region (northeastern Arizona, United States) and dated detrital sanidine sample locations. Red line shows the western part of the Crooked Ridge paleoriver pathway of Lucchitta et al. (2013) and corresponds to the profile in Figure 10. Fluvial upper Bidahochi Formation undivided is in orange with newly dated samples on Black Mesa and near Ganado, Arizona. The base of ca. 16 Ma lacustrine Bidahochi Formation is shown with a yellow line. Thermochronology samples show that rocks along the modern San Juan and Colorado Rivers were beneath 1–2 km of Mesozoic strata until after 6 Ma (Hoffman, 2009; Karlstrom et al., 2014). The main stem river incision points shown are discussed in Figure 10. AZ—Arizona; CA—California; CO—Colorado; ID—Idaho; NM—New Mexico; NV—Nevada; UT—Utah; WY—Wyoming; Lava Creek B WM—White Mesa locality for the 630 ka Lava Creek B ash.

Heizler_GES02319 1st pages / 2 of 17

in the past 2 m.y. near the confluence of the Colorado and Little Colorado Rivers.

Lucchitta and Holm (2019) doubted the <2 Ma age and reiterated their prior interpretation for an Oligocene–Miocene Crooked Ridge paleoriver. They argued that the Crooked Ridge River paleovalley could be substantially older than the alluvium within it, provided the 2 Ma age reported by Hereford et al. (2016) was accurate (which they doubted). Thus, the paleovalley dates to the "birth" (their terminology) of the Crooked Ridge River in the late Oligocene, whereas the alluvium records the "death" of that river, raising the possibility that this paleoriver and paleovalley system could have been "alive" in the study region for ~25 m.y.

The goals of this paper are: (1) to provide additional $^{40}Ar/^{39}Ar$ dating of detrital sanidine within the White Mesa alluvium and surrounding deposits, and (2) reexamine the geomorphic context of the deposits. Given the confusing terminology, we define the following features shown in Figure 1 as follows. Crooked Ridge and White Mesa, on the Kaibito Plateau of northeastern Arizona, are southwest-trending elevated and inverted geomorphic features (Fig. 1). The 17-km-long White Mesa stands with local, steep topographic relief of ~200 m. It exposes an ancient valley system with five tributary paleochannels filled with White Mesa alluvium. Crooked Ridge, whose topography is inverted by ~100 m, is a discontinuous gravel-capped ridge extending 32.5 km southwest from White Mesa that was part of the same Crooked Ridge paleoriver system. Two kilometers further southwest is "The Gap", a wind gap in the Echo Cliffs that has lag gravel consisting of pebbles and small cobbles, including rare granite and quartzite. This marks the downstream preserved end of the White Mesa alluvium and the Crooked Ridge paleoriver system (Fig. 1; Hereford et al., 2016).

METHODS

Detrital sanidine was dated from 18 samples, with 3530 total grains analyzed at the New Mexico Geochronology Research Laboratory (Socorro, New Mexico; Table 1). Sanidine is concentrated by handpicking crystals under a polarizing binocular microscope from the bulk K-feldspar population while the grains are immersed in wintergreen oil. Sanidine is distinguished by its lack of microtextures, such as perthite lamellae and turbidity, which are common in orthoclase and microcline. We also prepared a sanidine separation from the Red Lake tuff that is inset into the White Mesa alluvium and thus can be used to constrain a minimum deposition age using standard magnetic and heavy liquid methods. The samples were irradiated at either the U.S. Geological Survey TRIGA reactor (Denver, Colorado) or in the Oregon State University TRIGA reactor (Corvallis, Oregon) along with standard Fish Canyon Tuff sanidine (FC-2) with an assigned age of 28.201 Ma (Kuiper et al., 2008). The ^{40}K decay constant used for age calculation is 5.463×10^{-10}/a (Min et al., 2000). Argon gas was extracted almost exclusively by single-crystal laser fusion using a CO_2 laser, however some grains were step heated. Isotope measurements were done using a ThermoFisher Scientific ARGUS VI multicollector noble gas mass spectrometer. All age uncertainties are reported at 1σ and reflect analytical uncertainty only. Maximum depositional ages are generally derived by calculating the weighted inverse variance mean age of the youngest population of dates or, in some cases, are derived from a single analysis. Additional details regarding maximum depositional age calculations are given in the text, and complete analytical details along with supporting tables or isotopic results and metadata are provided in Table S1 in the Supplemental Material[1].

RESULTS OF DETRITAL SANIDINE AND TUFF DATING

We present new detrital sanidine results from four geologic units that include the Eocene–Oligocene Chuska Sandstone, the Miocene Bidahochi Formation, the Pleistocene White Mesa alluvium, and samples of terrace deposits along the present Colorado and San Juan Rivers (Fig. 1; Table 1). Additionally, detrital sanidine analysis was conducted on a remnant deposit from Black Mesa. We also directly dated the Red Lake tuff that is inset into the White Mesa alluvium. Detrital sanidine data derived from all 18 samples are generally dominated by ages between 40 and 20 Ma with an additional large population of grains of <2.5 Ma found in the Pleistocene units.

Samples of White Mesa alluvium were collected from the two main outcrops at White Mesa and Crooked Ridge (Fig. 1). Samples span from top to bottom stratigraphically (Fig. 2) and the entire preserved length of the paleoriver system (Fig. 1). Outcrop photos in Figure 3 show the excellent exposures and sampling pits dug to avoid contamination. Our new data set includes additional analyses of two samples (PR-AZ-3 and PR-AZ-4; Figs. 3A, 3C) from Hereford et al. (2016) that confirm maximum depositional ages of <2 Ma for both samples. The initial analysis of sample PR-AZ-3 included low-resolution step heating of 29 single grains, which demonstrates that argon loss did not occur, thereby supporting the common procedure of single-crystal laser fusion that is conducted for most sanidine geochronology studies (Schaen et al., 2020). For sample PR-AZ-3, we report 207 new detrital sanidine analyses, and for sample PR-AZ-4, we report 164 new analyses, such that when combined with the data of Hereford et al. (2016) the complete data sets have 311 and 261 total grains dated, respectively (Table 1). We found a similar proportion of ca. 2 Ma grains in this new effort. We now have 17 total grains in these two samples that are younger than 2.5 Ma, thereby greatly strengthening the initial claim of Hereford et al. (2016) that the White Mesa alluvium is early Pleistocene in age.

Three additional samples of the White Mesa alluvium are also reported here. Sample PR-AZ-5 was sampled from high in the Crooked Ridge section (Fig. 3D) near The Gap; it yielded 171 detrital sanidine dates with one grain at 1.955 ± 0.007 Ma. Sample PR-AZ-2 (Fig. 3B), from near the base of the White Mesa alluvium at the railroad quarry where Crooked Ridge and White Mesa join, produced 171 detrital sanidine grains with no grains younger than ca. 9 Ma. We note that both samples PR-AZ-2 and PR-AZ-5 are on average coarser grained than samples PR-AZ-3 and PR-AZ-4, which may have contributed to the lower proportion of Pleistocene detrital sanidine grains. Sample WM-2 (Fig. 3E) near

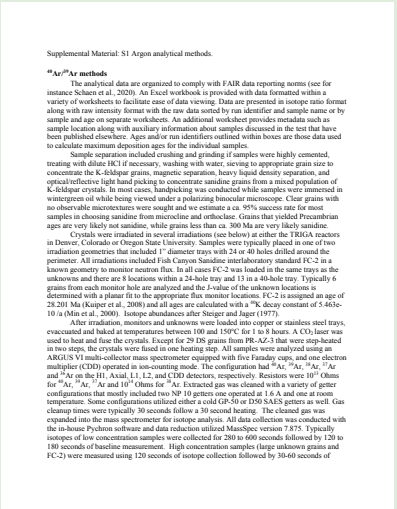

Supplemental Material: S1 Argon analytical methods.

$^{40}Ar/^{39}Ar$ methods

The analytical data are organized to comply with FAIR data reporting norms (see for instance Schaen et al., 2020). An Excel workbook is provided with data formatted within a variety of worksheets to facilitate ease of data viewing. Data are presented in isotope ratio format along with raw intensity format with the raw data sorted by run identifier and sample name or by sample and age on separate worksheets. An additional worksheet provides metadata such as sample location along with auxiliary information about samples discussed in the test that have been published elsewhere. Ages and/or run identifiers outlined within boxes are those data used to calculate maximum deposition ages for the individual samples.

Sample separation included crushing and grinding if samples were highly cemented, treating with dilute HCl if necessary, washing with water, sieving to appropriate grain size to concentrate the K-feldspar grains, magnetic separation, heavy liquid density separation, and optical/reflective light hand picking to concentrate sanidine grains from a mixed population of K-feldspar crystals. In most cases, handpicking was conducted while samples were immersed in wintergreen oil while being viewed under a polarizing binocular microscope. Clear grains with no observable microtextures were sought and we estimate a ca. 95% success rate for most samples in choosing sanidine from microcline and orthoclase. Grains that yielded Precambrian ages are very likely not sanidine, while grains less than ca. 300 Ma are very likely sanidine.

Crystals were irradiated in several irradiations (see below) at either the TRIGA reactors in Denver, Colorado or Oregon State University. Samples were typically placed in one of two irradiation geometries that included 1" diameter trays with 24 or 40 holes drilled around the perimeter. All irradiations included Fish Canyon Sanidine interlaboratory standard FC-2 in a known geometry to monitor neutron flux. In all cases FC-2 was loaded in the same trays as the unknowns and there are 8 locations within a 24-hole tray and 13 in a 40-hole tray. Typically 6 grains from each monitor hole are analyzed and the J-value of the unknown locations is determined with a planar fit to the appropriate flux monitor locations. FC-2 is assigned an age of 28.201 Ma (Kuiper et al., 2008) and all ages are calculated with a ^{40}K decay constant of $5.463e-10$ /a (Min et al., 2000). Isotope abundances after Steiger and Jager (1977).

After irradiation, monitors and unknowns were loaded into copper or stainless steel trays, evacuated and baked at temperatures between 100 and 150°C for 1 to 8 hours. A CO_2 laser was used to heat and fuse the crystals. Except for 29 DS grains from PR-AZ-3 that were step-heated in two steps, the crystals were fused in one heating step. All samples were analyzed using an ARGUS VI multi-collector mass spectrometer equipped with five Faraday cups, and one electron multiplier (CDD) operated in ion-counting mode. The configuration had ^{40}Ar, ^{39}Ar, ^{38}Ar, ^{37}Ar and ^{36}Ar on the H1, Axial, L1, L2, and CDD detectors, respectively. Resistors were 10^{13} Ohms for ^{40}Ar, ^{39}Ar, ^{37}Ar and 10^{14} Ohms for ^{38}Ar. Extracted gas was cleaned with a variety of getter configurations that mostly included two NP 10 getters one operated at 1.6 A and one at room temperature. Some configurations utilized either a cold GP-50 or D50 SAES getters as well. Gas cleanup times were typically 30 seconds follow a 30 second heating. The cleaned gas was expanded into the mass spectrometer for isotope analysis. All data collection was conducted with the in-house Pychron software and data reduction utilized MassSpec version 7.875. Typically isotopes of low concentration samples were collected for 280 to 600 seconds followed by 120 to 180 seconds of baseline measurement. High concentration samples (large unknown grains and FC-2) were measured using 120 seconds of isotope collection followed by 30-60 seconds of

[1]Supplemental Material. Geochronology data. Please visit https://doi.org/10.1130/GEOS.S.13585055 to access the supplemental material, and contact editing@geosociety.org with any questions.

TABLE 1. SUMMARY OF DETRITAL MINERAL DATING RESULTS

Unit	Sample	MDA	MDA error (1σ)	MDA_n	MSWD	n_{total}	$n_{0-2.5}$	$n_{2.5-20}$	n_{20-40}	$n_{>40}$	$\%_{20-40}$	DS	DZ
San Juan and Colorado River terraces	SJR-2	1.[illegible]8	0.008	15	1.63	259	17	4	171	67	66	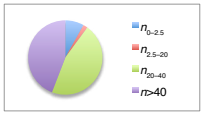	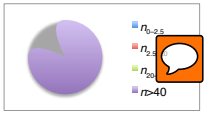
	POW-7A	!"#$!	0.20	1	NA	145	0	3	52	90	36		
	POW-14	0.679	0.006	47	1.14	220	53	4	95	68	43		
	POW-18	1.20	0.04	5	5.66	57	6	2	21	28	37		
	GLGC-T	8.95	0.03	1	NA	252	0	5	88	159	35		
Total DS						933	76	18	427	412	46		
DZ		57.1	0.9	1	NA	175	0	0	0	175	0		
White Mesa Alluvium	PR-AZ-2	9.00	0.01	3	4.27	171	0	7	137	27	80	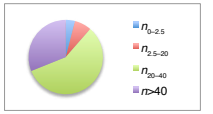	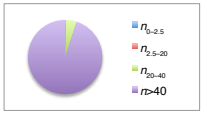
	PR-AZ-3	1.96	0.02	6	2.47	311	8	30	158	115	51		
	PR-AZ-4	1.92	0.02	6	1.31	261	9	21	147	84	56		
	PR-AZ-5	1.955	0.007	1	NA	171	1	15	97	58	57		
	WM-2	1.870	0.007	15	1.87	276	30	15	145	86	53		
Total DS						1190	48	88	684	370	58		
DZ		15	4	1		481	0	2	22	457	5		
BM	BM-1	9.052	0.003	71	5.1	232	0	111	94	27	41	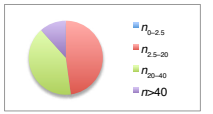	
Total DS						232	0	111	94	27	41		
Bidahochi Formation	%&'[illegible]	6.07	0.07	1	NA	181	0	15	124	42	69		
	%&'(&!)&+	6.31	0.02	1	NA	210	0	21	158	31	75	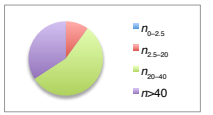	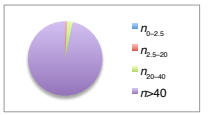
	%&'(&!)&,	7.17	0.06	1	NA	91	0	11	63	17	69		
	%&'(&!)&-	10.98	0.02	1	NA	167	0	18	17	132	10		
Total DS						649	0	65	362	222	56		
DZ		15.2	0.6	1		119	0	1	3	115	3		
Chuska Sandstone	CK-1	32.6	0.2	1	NA	268	0	0	40	228	15	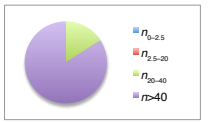	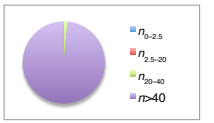
	CK-3	28.7	0.2	3	2.5	121	0	0	10	111	8		
	CK-5	27.65	0.02	1	NA	137	0	0	34	103	25		
Total DS						526	0	0	84	442	16		
DZ		27.5	0.5	6	1.88	402	0	0	6	396	1		

Total DS grains 353

Total DZ grains (from Hereford et al. 2016) 1177

MDA—maximum depositional age (in Ma)

MDA_n—number of dates defining maximum depositonal age

MSWD--mean square [illegible]ed deviation

$n_{0-2.5}$—number of date[illegible] 5 Ma

$n_{2.5-20}$—number of dates >2.5 and ≤20 Ma

n_{20-40}—number of date[illegible]nd ≤40 Ma

$n_{>40}$—number of date[illegible]a

$\%_{20-40}$—percentage of dates >20 and ≤40 Ma

NA—not applicable.

DS—detrital sanidine

DZ—detrital zircon

BM—Black Mesa

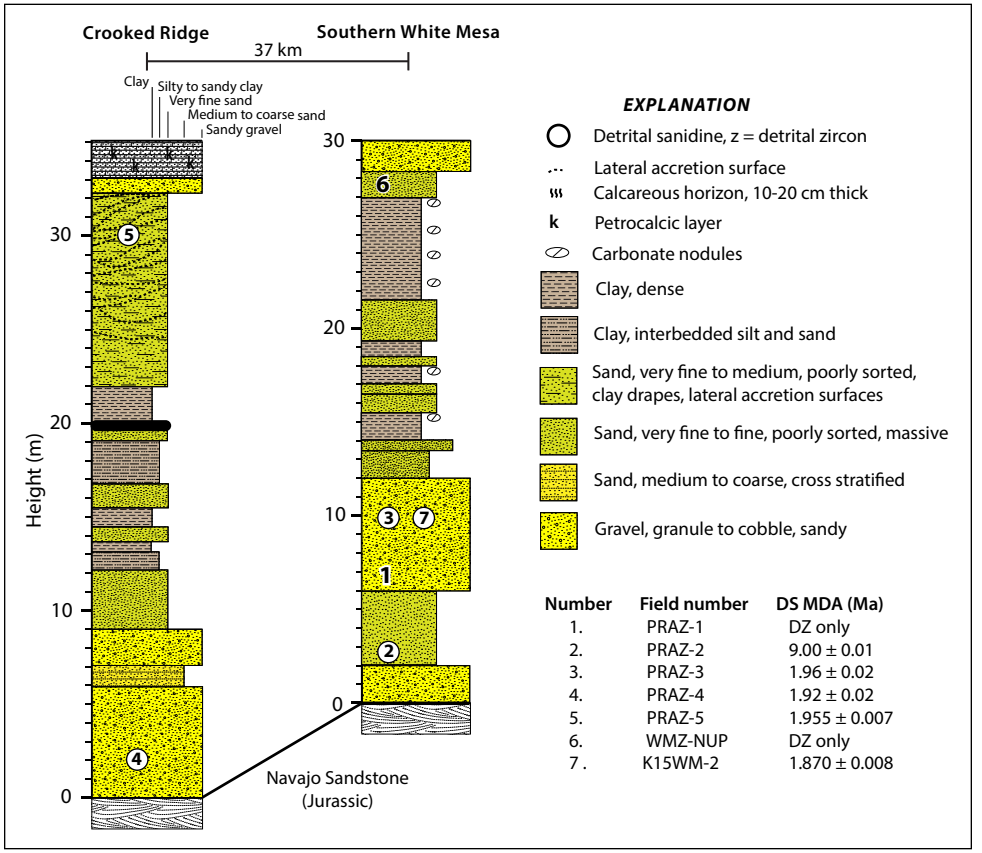

Figure 2. Composite stratigraphic sections and sampling locations for the White Mesa alluvium (modified from Hereford et al., 2016). New detrital sanidine samples are WM-2, PR-AZ-2, and PR-AZ-5. Samples with both detrital zircon and detrital sanidine are PR-AZ-2, PR-AZ-3, and PR-AZ-4. DS—detrital sanidine; DZ—detrital zircon; MDA—maximum depositional age.

the base of the west margin of the trunk channel on White Mesa produced 276 grains, with 39 being younger than 2.5 Ma (Table 1). In total, 119 detrital sanidine grains were analyzed from the White Mesa alluvium with 48 crystals (4%) yielding ages <2.5 Ma. All of the White Mesa alluvium samples contain numerous 40–20 Ma grains (58%).

We also sampled other Cenozoic sands and sandstones in the region for comparison of detrital sanidine age populations (Fig. 1; Table 1). Four terraces were sampled from different heights above the present Colorado River just downstream of its San Juan River confluence in Glen Canyon and along one terrace near Bluff, Utah, on the present San Juan River. These reflect the detrital sanidine composition over the past 1–2 m.y. based on analysis of 933 grains. Three of these samples have multiple detrital sanidine grains that are <2.5 Ma; however, all are generally enriched with 40–20 Ma sanidine.

One sample (BM-1) was taken from a thin remnant deposit of sand and gravel on Black Mesa (Fig. 3F), from which we dated 232 crystals. This sample has a subequal number of dates that fall between 40 and 20 Ma and 20–9 Ma and yielded a maximum depositional age of ca. 9 Ma (Table 1). Four samples were taken of uppermost Bidahochi Formation at four localities near Ganado, Arizona. A total of 649 crystals were dated; all have sparse young populations of 11–6 Ma grains, and three samples are enriched (~70%) in 40–20 Ma detrital sanidine. Three samples of Chuska Sandstone were taken of the eolian upper Chuska Sandstone from which 527 crystals were dated. The majority of grains are older than 40 Ma. However, two of the three detrital sanidine samples contain ~20% grains <40 Ma (Table 1). The Chuska samples, in contrast to the other samples, have a large population of Precambrian grains that are likely non-sanidine K-feldspars (i.e., orthoclase or microcline) (Table S1 [footnote 1]).

The detrital sanidine data contrast strongly with the published detrital zircon data in Hereford et al. (2016). The detrital zircon populations contain a large portion of grains older than 40 Ma, with only 31 of 1177 (~2.6%) ranging between 40 and 20 Ma and none younger than ca. 15 Ma (Table 1). These contrasting results demonstrate the utility of detrital sanidine analysis for volcaniclastic and tephra-bearing Cenozoic deposits, particularly in providing more accurate and precise maximum depositional ages and obtaining specific provenance determinations. Combined, detrital sanidine and detrital zircon analyses can define the full spectrum of source ages and should be viewed as complimentary methods, each having specific strengths.

The Red Lake tuff, deposited in an alluvial gravel on Jurassic Navajo Sandstone, occupies a geomorphic position below White Mesa, and this inset relationship provides a minimum age of the White Mesa alluvium. This tuff has a sparse and very fine-grained crystal population and thus was challenging for mineral separation and dating. Thirty-eight (38) single crystals were analyzed; 14 were sanidine (Fig. 4). The remainders are either quartz or plagioclase and were omitted from further consideration. The eight youngest crystals define a normal distribution and yield a weighted mean age of 1.07 ± 0.05 Ma, with six older grains falling between ca. 211 and 2.2 Ma. This indicates that the White Mesa alluvium is no older than ca. 1.1 Ma.

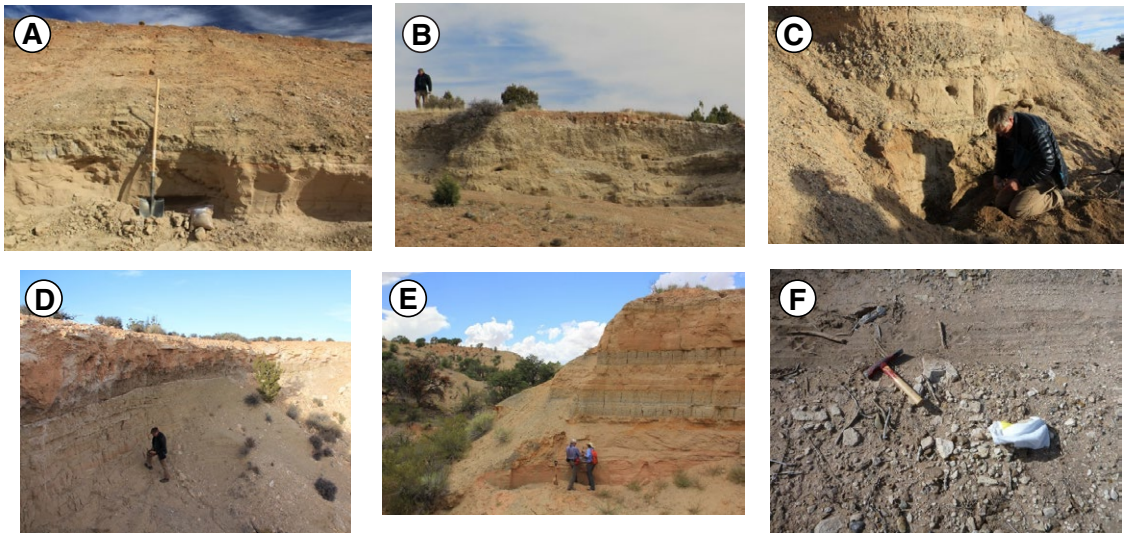

Figure 3. Photos of field exposures sampled for this study (see Fig. 1 for locations). (A) Sample PR-AZ-3: Highway road cut; had 8/311 grains <2.5 Ma and a maximum depositional age (MDA) of 1.96 ± 0.02 Ma. (B) Sample PR-AZ-2: Lower Railroad Quarry; had 0/171 grains <2.5 Ma and a MDA of 9.00 ± 0.01 Ma. (C) Sample PR-AZ-4: Near The Gap, low in section along Crooked Ridge; had 9/261 grains <2.5 Ma and a MDA of 1.92 ± 0.02 Ma. (D) Sample PR-AZ-5: The Gap, high in section; had 1/172 grains <2.5 Ma and a maximum depositional age of 1.955 ± 0.007 Ma. (E) Sample WM-2: On White Mesa, west margin of trunk valley; had 30 grains < 2.5 Ma and a MDA of 1.87 ± 0.008 Ma. (F) Sample BM-1: Thin remnant deposit on Black Mesa; had 0/232 grains <2.5 Ma but a large population of 9 Ma grains suggesting it may be coeval with a tephra of this age; its MDA is 9.052 ± 0.003 Ma.

Maximum Depositional Ages

Maximum depositional ages (MDAs) are reported for all samples (Table 1). There is significant debate in detrital zircon studies about what set of analyses defines the MDA (e.g., Gehrels, 2014; Coutts et al., 2019; Copeland, 2020), and those considerations apply to detrital sanidine studies as well. Herein, where a single grain is significantly younger than other grains at 2σ uncertainty, this single grain age is used to define the MDA. For the majority of the White Mesa alluvium and present San Juan River samples, the MDA is defined by the youngest several dates that yield a normal distribution, based on the mean square weighted deviation (MSWD) value, which also considers the number of grains in the distribution. Thus, the MSWD that defines a population at the 95% confidence interval has a window of values that is a function of *n* (Mahon, 1996). Figures 5A and 5B demonstrate selection of grains to define the MDA for samples WM-2 and BM-1, whereas the analyses that define the MDA for all samples can be found in Table S1 (footnote 1). Factors such as radiogenic yield and K/Ca values can help guide the choice of the youngest population.

For sample WM-2, there are 30 detrital sanidine grains younger than 2.5 Ma, and based on the method described above, 15 are used to define a MDA of 1.870 ± 0.007 Ma (Fig. 5A). Data are arranged in order of increasing age, and using the MSWD criteria that consider both analytical uncertainty and degrees of freedom, we identify the greatest number of grains that define the youngest normal distribution of dates. In this case, the youngest 10 dates yield a normal distribution; however, with addition of the next oldest grain to the distribution, the MSWD is too elevated, and thus this grain is rejected in the MDA calculation. However, the age of the 12th-youngest grain is included because its uncertainty is relatively high and thus it cannot be analytically distinguished from the ages of the 10 youngest grains. This is also true for several of the older grains with higher uncertainties, and thus they are included in the MDA. This analysis assumes that there is no argon loss in the crystals defining the MDA and that analytically older crystals either come from an older source rock or have excess argon that can be hosted in melt inclusions within sanidine crystals.

The grains with ca. 9 Ma dates from sample BM-1 from Black Mesa (Fig. 5B; Table 1) have very high precision related to their age, size, and high radiogenic yields. Of the 94 crystals that are <10 Ma, 71 were chosen to define an MDA of 9.052 ± 0.003 Ma. However, this data set has a somewhat elevated MSWD value of 5.1 indicating some excess scatter. Rather than cull the data to a very low *n* to achieve a lower MSWD, we accept that there is no unambiguous method to fully parse out sources of scatter. For instance, the high-precision results might be resolving small differences in neutron flux, there could be minor geological disturbance (argon loss, excess argon), and/or some grains may be from a slightly older source. Importantly, the choice of the exact number of grains to include does not affect our conclusion, as obviously a MDA of ca. 9 Ma is far different from a MDA of ca. 2 Ma.

Table 1 summarizes the MDA values for all of the samples. For the White Mesa alluvium, we now have four samples with MDA between 1.96 ± 0.02 and 1.870 ± 0.007 Ma that are individually defined by one to 15 crystals. This substantially increases the MDA constraints reported by Hereford et al. (2016), which relied on two samples each with two grains to define the MDA. One sample (PR-AZ-2) did not yield any Pleistocene grains and has a MDA

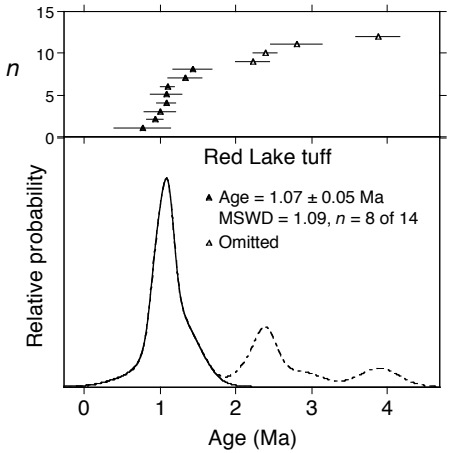

Figure 4. Age probability diagram for single-crystal sanidine results from Red Lake tuff. Dates are arranged in age-increasing pattern, with solid symbols representing the analyses chosen to derive the weighted mean age. Eight of 14 grains define the youngest population at 1.07 ± 0.05 Ma. Older grains are inherited either during eruption at the source or during post-depositional reworking. Two grains older than 4 Ma are not shown in the figure. Solid line represents the probability function for the 8 analyses defining the eruption age whereas the dashed line is the full probability function for all analyses younger than 4 Ma. Error bars are shown at 1σ . MSWD—mean square weighted deviation.

of 9.00 ± 0.01 Ma. The MDAs for the present-day Colorado River terraces fall between 10.4 Ma and 0.679 Ma, with two of the samples yielding robust MDAs ≤1.2 Ma. The San Juan River terrace from Bluff, Utah, has a MDA of 1.208 ± 0.008 Ma based on 15 grains. The Black Mesa sample, BM-1, has a large number of grains defining a MDA of 9.052 ± 0.003 Ma. The Bidahochi Formation samples have a limited number of crystals that are <10 Ma, and the MDA of these samples is defined by a single grain for each that range from ca. 11 to ca. 6 Ma (Table 1). Like the Bidahochi, the eolian Chuska Sandstone samples have a small number of dated grains that define MDAs between 32.6 ± 0.2 and 27.65 ± 0.02 Ma. These fall within the known 33–27 Ma depositional age range of the Chuska Sandstone (Cather et al., 2008).

Full Detrital Sanidine Age Distributions

In order to show comparative aspects of the detrital sanidine data between the sampled units, the data are organized in five geological groups at various age ranges (Fig. 6). Figure 6A shows the four geological groups for the detrital sanidine data that fall between 20 and 0 Ma. The Bidahochi Formation shows multiple modes between 19 and 6 Ma, whereas the Black Mesa remnant deposit is dominated by a 9 Ma mode with an additional scattering of ages between 18.7 and 10 Ma. The composite graph for the White Mesa alluvium in Figure 6A shows a prominent clustering of <2 Ma grains that is dominated by the sample WM-2. This composite also reveals multiple modes between 20 and 4 Ma and a prominent mode at ca. 9 Ma. In the 20–0 Ma age range, the present Colorado River terraces show a concentration of grains <1.2 Ma that is dominated by the large number of 0.68 Ma crystals derived from sample POW-14. There are relatively few Miocene ages from these terraces in comparison to the other samples. Figure 6B shows the 20–0 Ma grains for individual samples and demonstrates overall consistency of the individual samples within the geological units.

Figure 6C examines the 40–20 Ma detrital sanidine grains in the four groups shown in Figures 6A but includes the Chuska Sandstone samples as well. Overall, there is remarkable similarity of the age distribution between the sample groups with prominent modes near 35–34, 32, 30–27, and 23 Ma. The cumulative number of grains that fall in this age range is ~1651, nearly half (47%) of the total (3530) detrital sanidine grains dated; this dwarfs the number of lower-precision detrital zircon dates of this age range (n = 31; 2.6%; Hereford et al., 2016). Individual samples exhibit 40–20 Ma detrital sanidine populations that are 8%–80% of total grains for the Bidahochi Formation, Black Mesa, White Mesa alluvium, and Colorado River and San Juan River terraces (Table 1). The Chuska Sandstone samples have comparatively fewer crystals (8%–25%) of this age. The individual samples shown in Figure 6D reveal that most samples share similar modes, demonstrating the general consistency for individual samples within and between geological units that range widely in age.

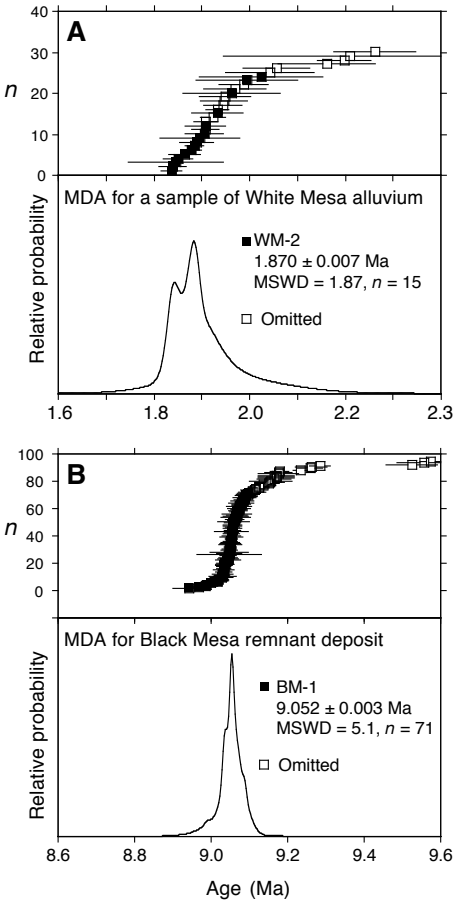

Figure 5. Relative probability diagrams for two detrital sanidine samples showing methods of analyses used to define the maximum depositional age (MDA). Dates are arranged in age-increasing pattern, with solid symbols representing the analyses chosen to derive the weighted mean age. (A) The maximum depositional age is given by the data set that the yields the youngest age and has a mean square weighted deviation (MSWD) value that falls within the 95% confidence window for a given n. (B) The same process as in A, however the MSWD value can be higher as some excess age scatter may be attributed to neutron flux gradients and/or geological factors such as derivation of grains from a slightly older source.

NOTE: I made the size of the x,y labels in Figure 6 smaller as they were quite a bit larger than other text.

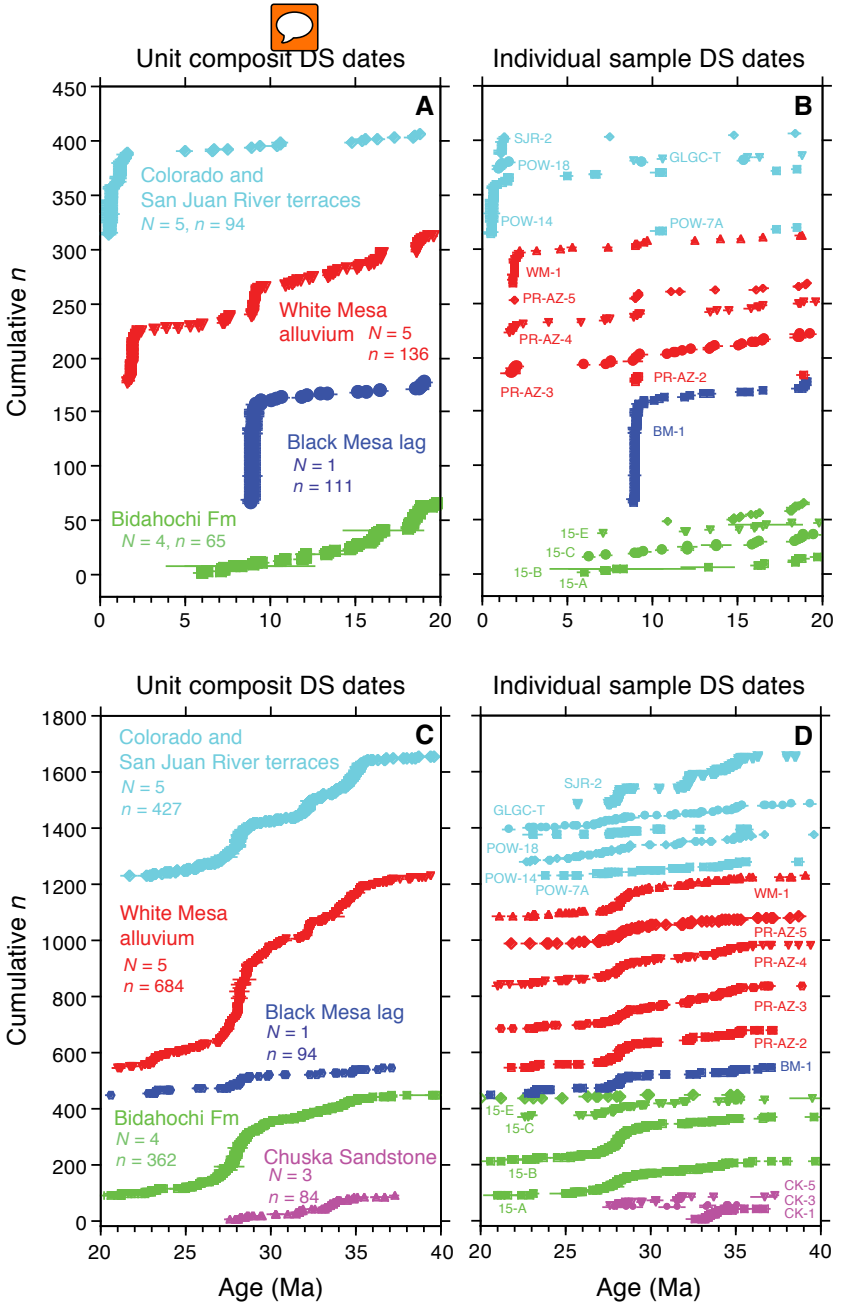

Figure 6. (A,B) Summary of 0–20 Ma detrital sanidine grains from the study area. (A) Composite summary of young grains grouped by unit. Cyan—young grains from terraces of the present Colorado and San Juan Rivers with a high proportion of <1 Ma grains; Red—composite of all five White Mesa alluvium samples showing 1.9 Ma maximum depositional age (*n* = 48 at ca. 2 Ma grains) as well as a significant 9 Ma mode; blue—Black Mesa remnant deposit sample that is dominated by 9 Ma grains; green—composite of four new Bidahochi Formation samples from near Ganado, Arizona. (B) Granular stack of young grains from individual samples; note significant number of ca. 2 Ma grains from four out of five White Mesa alluvium samples and the presence of ca. 9 Ma grains in all samples. (C,D) Summary of 20–40 Ma detrital sanidine grains. (C) Groupings as in A with addition of Chuska Sandstone (purple). All show probable San Juan volcanic field–derived sanidine grains. (D) Granular stack of grains from individual samples; most individual samples show a near-continuum of 20–40 Ma sanidine ages with discrete breaks between individual ignimbrite sources. Error bars shown with horizontal lines represent 1σ uncertainty. Sample names of Chuska Sandstone samples are abbreviated where beginning numbers of 8–27 are omitted.

INTERPRETATION OF DETRITAL SANIDINE DATA

In each of the composite age groups of Figure 6A, the near continuum of post–20 Ma sanidine raises the likelihood that maximum depositional ages approximate true depositional ages in some samples. Each of the White Mesa alluvium samples except PR-AZ-2 contains 1.89–2.5 Ma sanidine. The White Mesa alluvium was sampled at five outcrops from both Crooked Ridge and White Mesa, including samples from the top and bottom of the unit. These localities are representative of the entire 57-km-long Crooked Ridge paleoriver. This lays to rest any doubts cast by Lucchitta and Holm (2019) of the prior detrital sanidine study of Hereford et al. (2016) that reached the same conclusion using fewer dated grains; it also argues against the confusing assertion that Crooked Ridge paleoriver deposits are different than White Mesa alluvium (Lucchitta and Holm, 2019, p. 540 and 543).

Lucchitta et al. (2013) suggested that ~4% of their clasts in the White Mesa alluvium were derived from the San Juan volcanic field that is

located in SW Colorado. Hereford et al. (2016) confirmed the existence of San Juan volcanic field detritus based on the presence of detrital zircons of this age as well as abundant Eocene to Oligocene detrital sanidine grains. Combined, these data sets support the interpretation that exotic clasts, some zircon, and a multitude of sanidine grains in the White Mesa alluvium were ultimately derived largely from the San Juan Mountains. Hereford et al. (2016) noted a prominent age mode of detrital sanidine grains at 28.2 Ma and correlated it to the voluminous Fish Canyon Tuff of the San Juan Volcanic Field. With now >680 detrital sanidine grains in the 40–20 Ma age range from the White Mesa alluvium, we expand the work of Hereford et al. (2016) to convincingly show that multiple discrete detrital sanidine modes can be correlated to specific San Juan volcanic field ignimbrites.

Figures 7A and 7B compare sanidine age and K/Ca data from the San Juan Volcanic Field to detrital sanidine data from the White Mesa alluvium that is given in Figures 7C and 7D. Although comparison of detrital sanidine age modes with reported ignimbrite ages is an effective means to determine potential source calderas, correlations are enhanced by utilizing the K/Ca value of the sanidines, which is derived from the measured $^{39}Ar/^{37}Ar$ ratio of each detrital sanidine grain. The detrital sanidine data are compartmentalized into age ranges of 38–31 Ma and 29.5–26.5 Ma in order to visually resolve discrete modes. K/Ca values and age data are given for individual detrital sanidine grains and for single-crystal sanidine ages for various San Juan volcanic field rocks. The ignimbrite data are primarily taken from Lipman and McIntosh (2008) and Lipman et al. (2015), as well as some data from the New Mexico Geochronology Research Laboratory database (https://maps.nmt.edu). For ignimbrites, Figures 7A and 7B show discrete age-K/Ca populations that define regions outlined by the ellipses, with each ellipse identified by ignimbrite name. These ellipses are overlain on the detrital sanidine data in Figures 7C and 7D to show the excellent correspondence of many detrital sanidine age-composition modes.

This analysis identifies at least 10 major San Juan volcanic field eruptions between 29.5 and 26.5 Ma that contributed to the White Mesa alluvium detrital sanidine population (Fig. 7A). We note that this high-fidelity record could not be obtained from detrital zircon analyses due to limitations of detrital zircon precision and the low concentration of detrital zircon grains of this age range. The time span from 38 to 31 Ma identifies multiple San Juan volcanic field eruptions such as the Bonanza, Badger Creek, and Wall Mountain Tuffs (Fig. 7B). There are also some prominent modes that may be from

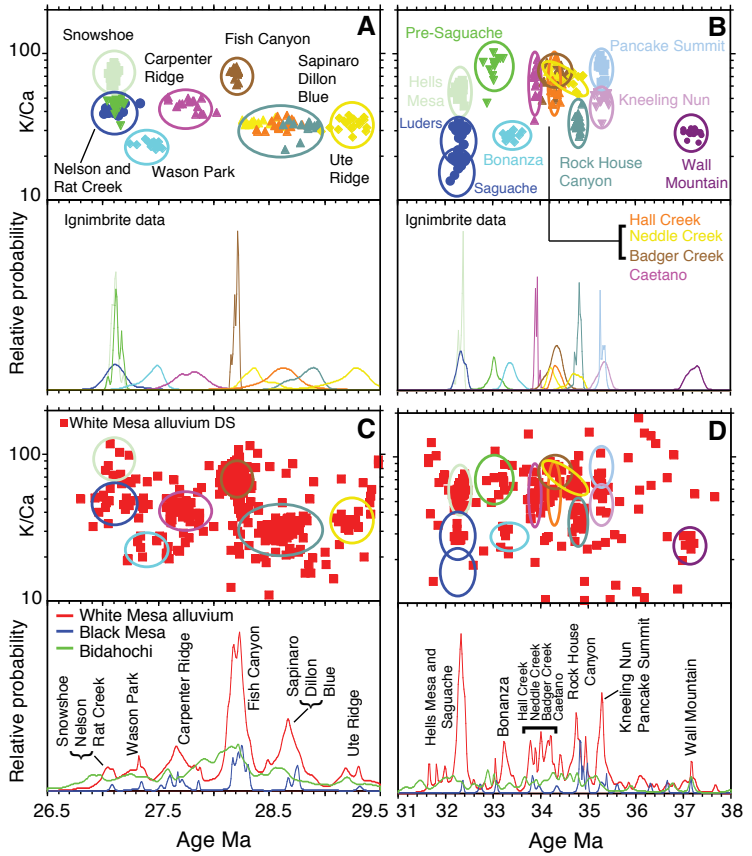

Figure 7. Multidimensional scaling analysis of age and K/Ca values for two age ranges, demonstrating discrete groups that correlate to San Juan volcanic field ignimbrites (Lipman and McIntosh, 2008; Lipman et al., 2015). (A,B) Single-crystal sanidine dating results from various ignimbrites mainly from the San Juan volcanic field with some also from the Mogollon-Datil volcanic field (Henry and John, 2013) and Nevada calderas (Henry and John, 2013). (C,D) Detrital sanidine data from White Mesa alluvium, overlain with ellipses defined by data shown in A and B. Discrete age-K/Ca populations strongly correlate to the ignimbrite data, demonstrating major modes in the detrital sanidine distribution that ultimately derive from the San Juan volcanic field. Shown in the lowest panels are the age probability plots for the White Mesa alluvium (red), Black Mesa remnant deposit (blue), and the Bidahochi Formation (green). Multiple discrete age modes are observed in all sample groups.

Mogollon-Datil volcanic field (central New Mexico) eruptions such as the Hells Mesa, Rock House Canyon, and Kneeling Nun Tuffs (see McIntosh et al., 1992). There are other detrital sanidine modes, especially in the 34–35 Ma range, that are not readily linked to either the San Juan volcanic field or Mogollon-Datil volcanic field. We include some data from large ignimbrites from Nevada (Caetano, Hall Creek, Pancake Summit Tuffs; cf. Henry and John, 2013) as possible sources, however occurrence of grains within the White Mesa alluvium from these tuffs is quite speculative. It is possible that sanidine from other volcanic sources is recorded in the detrital sanidine record, such as now-eroded parts of the San Juan volcanic field or poorly characterized parts of the Marysvale volcanic field of Utah. We interpret that most or all of the 11 Ma to present fluvial units in our study area contain a significant proportion of grains that were ultimately derived from the San Juan volcanic field. The ubiquitous presence and high percentage of these grains suggests that San Juan Mountains–derived detritus was repeatedly recycled into sedimentary systems of many ages, including the ca. 33–27 Ma upper Chuska Sandstone, ca. 16–6 Ma Bidahochi Formation, ca. 2 Ma White Mesa alluvium, and the various Pleistocene terraces of the present Colorado and San Juan Rivers.

The ca. 16–6 Ma Bidahochi Formation (Dallegge et al., 2003) marks the principal episode of aggradation on the southwestern Colorado Plateau since regional, post-Chuska exhumation began ca. 27 Ma (Cather et al., 2008). The maximum thickness of the Bidahochi Formation is ~240 m (Love, 1989). The sub-Bidahochi erosion surface dips southwest and ranges in elevation from ~1830 m at Hopi Buttes located in northern Arizona to ~2255 m south of Gallup, New Mexico (Dickinson, 2013). The remnant deposits on Black Mesa (elevation ~2230 m) contain exotic pebbles (~8% with San Juan volcanic field and Needle Mountains [Colorado] affinity; Lucchitta et al., 2013). Sanidine in the remnant deposits on Black Mesa was derived dominantly from the San Juan volcanic field. The maximum depositional age of this deposit (ca. 9 Ma) suggests it may be a remnant of the much-eroded Bidahochi Formation, as shown in Figure 1.

Black Mesa is a topographically inverted Laramide basin. Prior to the onset of post-Chuska erosion, it contained a significant thickness of post-Santonian Cretaceous strata in addition to the overlying Chuska Sandstone such that the total thickness of missing strata is as much as ~1 km (Cather et al., 2008, their figure 14). If the remnant deposits on Black Mesa are indeed equivalent to the Bidahochi Formation, then most of the missing strata were eroded prior to Bidahochi sedimentation. If so, then in the nearby White Mesa to The Gap area, at most only a few hundred meters of post-Bidahochi erosion occurred prior to deposition of the ca. 2 Ma White Mesa alluvium. This proposed new location for preserved Bidahochi Formation is reasonable given the known distribution of fluvial Bidahochi Formation on the southwest-dipping paleodepositional slope tributary to the Little Colorado paleoriver (Dickinson, 2013). Its lack of preservation except for this remnant on Black Mesa may reflect the northward increase in post–6 Ma depth of exhumation of this part of the Colorado Plateau (Cooley et al., 1969, p. A1; Karlstrom et al., 2017). Considering the typical gradient of the Bidahochi Formation in areas to the south (~3.5 m/km), it is likely that the Crooked Ridge paleoriver, with its steeper gradient (average 7 m/km; Hereford et al., 2016), intersected, and headed on, the eroding Bidahochi-age paleosurface in the vicinity of Skeleton Mesa (Fig. 1). Recycling may thus explain how San Juan volcanic field sanidine was inherited from the now-eroded Bidahochi Formation and incorporated into the White Mesa alluvium without requiring a major river headed in the San Juan Mountains at ca. 2 Ma as proposed by Lucchitta and Holm (2019).

As previously noted by Hereford et al. (2016), the Chuska Sandstone probably was not the major source of San Juan volcanic field–age detritus observed in the White Mesa alluvium. Although the upper part of the Chuska Sandstone does contain 28.2 Ma detrital sanidine grains from the Fish Canyon Tuff and possible other 33–38 Ma detrital sanidine grains derived from the San Juan volcanic field (Figs. 6C, 6D), they are not overly abundant and therefore cannot explain the much greater abundance of such detritus in the Bidahochi Formation and the White Mesa alluvium. As noted by Dickinson et al. (2010) based on detrital zircon analysis, the vast majority of the eolian Narbona Pass Member of the Chuska Sandstone was derived from the Mogollon Highland of southern Arizona. Lucchitta and Holm (2019, p. 537), however, concluded that: "The sandstone petrography shows that the Deza and Narbona Pass Members are identical in principal components and probably had similar sources, so no material in the Chuska Sandstone was derived from the San Juan Mountains…" This is incorrect as shown by paleocurrent data from the Chuska Sandstone type section in the southeastern Chuska Mountains, where approximately the upper two-thirds of the fluvial Deza Member (upper Eocene) was derived from the north-northeast (Repenning et al., 1958; Cather et al., 2003) and had a source in the San Juan Mountains. Moreover, none of the petrographic data for the Deza Member presented by Dickinson et al. (2010), and cited by Lucchitta and Holm (2019, their figure 8) in support of their above conclusion, were from the north-derived part of the Deza section, but rather were from stratigraphically lower, locally derived parts of the Deza Member. Petrographic data for two samples of the north-derived part of the Deza Member were described by Cather et al. (2003); these samples are compatible with derivation from the Laramide San Juan uplift (now exposed underneath the western half of the San Juan Volcanic field), the southwestern part of the Colorado Mineral Belt of southwest Colorado, and the nascent San Juan volcanic field. No detrital zircon or detrital sanidine analyses have yet been undertaken for the north-derived, upper part of the Deza Member.

As shown by inspection of the detrital sanidine age data, there is general similarity of the 40–20 Ma populations for the Bidahochi Formation, the White Mesa alluvium, and terrace samples, however this similarity can be further quantified. Figure 8A is a pairwise dissimilarity matrix showing Kolmogorov-Smirnov (K-S) test *D* statistic values that quantifies the degree of relative dissimilarity between any two pairs for the dominant 40–20 Ma cumulative grain populations. The *D* statistic is calculated as the maximum absolute difference between cumulative distributions (Massey, 1951). For example, every sample has a *D* statistic value

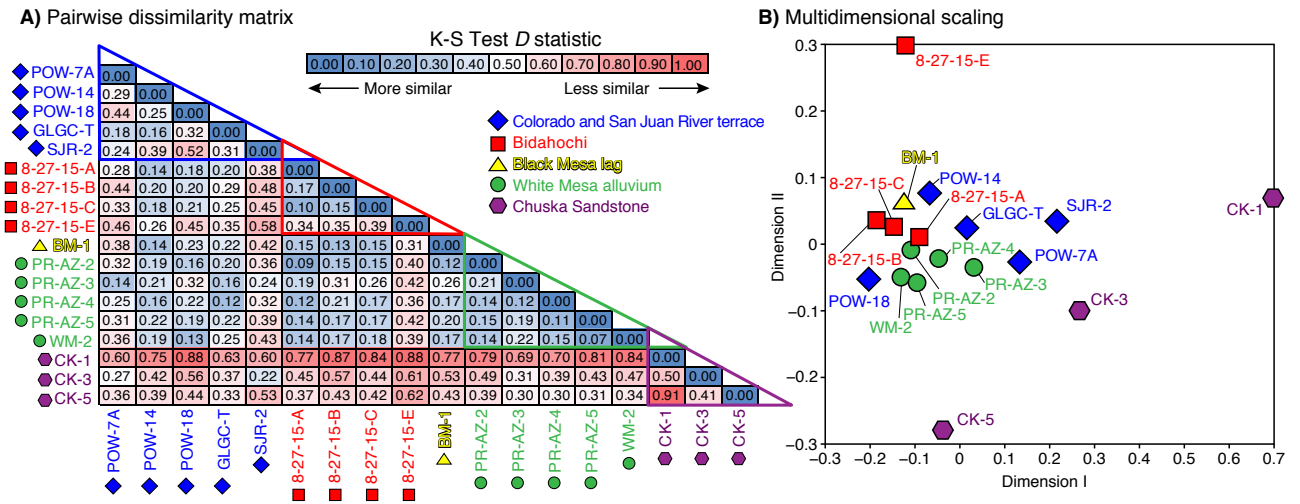

Figure 8. (A) Kolmogorov-Smirnov (K-S) test *D* statistic values for studied samples shown as a pairwise dissimilarity matrix from quantitative comparison of 40–20 Ma detrital sanidine age distributions, generated with DZstats version 2.3 for macOS (Saylor and Sundell, 2016). Note that larger numbers and hotter colors indicate higher dissimilarity. (B) Quantitative comparison results from A visualized using multidimensional scaling, generated using DZmds (Saylor et al., 2018). Multidimensional scaling transforms dissimilarity into distance in Cartesian space (here in two dimensions) via linear transformation and iterative rearrangement, seeking to minimize the misfit (stress) between distance and disparity. Larger distances correspond to greater dissimilarity. Stress is normalized by the sum of the squares of the interpoint distances. Low stress (e.g., <0.1) indicates a reasonable transformation; here stress is 0.053. We implement Kruskal's method for nonmetric multidimensional scaling (Kruskal, 1964), wherein dissimilarity is converted to distance via isotonic regression. The Euclidean distances have approximately the same rank as the dissimilarities and approximate a monotonic transformation. In panels A and B, blue corresponds to Colorado and San Juan River terraces, red to Bidahochi Fm., yellow to Black Mesa lag, green to White Mesa alluvium, and purple to Chuska Sandstone.

of zero with itself as is highlighted dark blue (i.e., the maximum absolute difference of two identical cumulative distributions is always zero), whereas higher *D* statistic values (greater difference between cumulative distributions) are shown in lighter blue through red tones. Groups of samples in Figure 8A are highlighted in triangles outlined with the same colors as their sample names. Figure 8B is a multidimensional scaling (MDS) plot generated by converting the pairwise dissimilarity matrix into distance and plotting in two-dimensional Cartesian space (e.g., Vermeesch, 2013). In this plot, samples that plot close together have a smaller K-S test *D* statistic values than those that plot farther apart.

Both plots show that samples of the White Mesa alluvium are similar to each other; K-S test *D* statistic values in Figure 8A are low, ranging from 0.07 to 0.22, and samples form a point cluster in MDS space in Figure 8B. Colorado and San Juan River terrace samples have a similar range of *D* values when compared to each other (0.16–0.52) as when compared with the White Mesa alluvium (0.12–0.43), as might be expected given diverse source regions tapped by these rivers. Three of the four Bidahochi samples (except 8-27-15E, which has a large component of Triassic detrital sanidine) are similar to each other (0.10–0.17) and also similar to the White Mesa alluvium (0.09–0.31). Chuska Sandstone has the largest *D* values, both internally (0.41–0.91) as well as when compared to all the other samples (0.22–0.88). These plots reinforce the conclusion that detrital sanidine of the White Mesa alluvium could have been recycled from Bidahochi Formation and that the Bidahochi Formation, White Mesa alluvium, and Colorado and San Juan River terraces all have similar age modes of 20–40 Ma grains that were ultimately derived from the San Juan Mountains. The precision of the detrital sanidine dating combined with the statistical power of MDS analysis offers rich potential for future matching of different detrital sanidine populations with distinct caldera eruption sources to inform more detailed future provenance analysis.

GEOMORPHIC EVIDENCE

Here we examine the geomorphic evidence that further rebuts the model for a hypothetical Oligocene to early Miocene river in the Crooked Ridge area that drained the San Juan Mountains and the notion that the <2 Ma White Mesa alluvium filled an older hypothetical paleovalley (Lucchitta and Holm, 2019). Instead, we make the case that the Crooked Ridge paleoriver was a local tributary to the Little Colorado River during the early Pleistocene, similar in scale and gradient to present-day Moenkopi

NOTE:
I added shading to Table 2—Ithoughtitwould help the reader since there is a lot of paragraph text. Please confirm this is okay.

Wash. To minimize repetition of previously published arguments, our responses that challenge the assertions of Lucchitta and Holm (2019) are summarized in Table 2.

Figure 9 shows the cross-sectional scale of the White Mesa alluvium paleovalley at White Mesa. As summarized by Hereford et al. (2016), sedimentologic and fossil evidence suggests that the White Mesa alluvium was deposited by a low-energy, suspended-sediment fluvial system with abundant fine-grained overbank deposits, rather than a vigorous braided river with distant headwaters. The White Mesa alluvium paleovalley was carved into Mesozoic rocks without evidence of inset relationships into older alluvial deposits. This paleovalley is broad, shallow, and of low relief and conforms to the observed White Mesa alluvium; any once-larger hypothetical paleovalley is speculative. Following abandonment of the White Mesa paleovalley, regional landscape lowering of ~125 m took place across the steep southeastern face of White Mesa at <0.8 Ma, as shown by the lower landscape position of the ca. 1.1 Ma Red Lake tuff.

Figure 10 shows the profile of the Crooked Ridge paleoriver near the drainage divide between modern trunk rivers of the Colorado, Little Colorado, and San Juan Rivers. This figure, plus the confirmed <2 Ma age of the White Mesa alluvium, argues against the model of Lucchitta and Holm (2019) that the headwaters of the hypothetical Crooked Ridge River were pirated by an ancestral San Juan River. Instead, incision rate data from San Juan River terraces above Bluff, Utah (location D of Fig. 10), show that the San Juan River was in its present course and only 140 m above today's channel at ca. 1.2 Ma, ~840 m below the hypothesized beheaded end of the White Mesa alluvium on White Mesa.

Figure 11 summarizes our alternative interpretation to explain the <2 Ma age of the White Mesa alluvium, the abundant San Juan Mountains–derived detritus, and the geomorphic context of the Crooked Ridge paleoriver. The 7 m/km gradient of the profile of the Crooked Ridge paleoriver is compared with the lower gradient (3.5 m/km regionally) of the Black Mesa profile, which is interpreted to be the base of the Bidahochi Formation. The ca. 2 Ma Crooked Ridge paleoriver is interpreted here to have intersected the eroding Bidahochi paleosurface in the vicinity of Skeleton Mesa, where it locally incorporated San Juan volcanic field sanidine and exotic pebbles from the Bidahochi Formation, which may have received sediment from the San Juan Mountains directly or reworked a now-eroded remnant of the San Juan volcanic field apron in the Four Corners area (the San Juan volcanic field undoubtedly extended well beyond its present extent; e.g.,

TABLE 2. SUMMARY OF RECENT INTERPRETATIONS OF THE HYPOTHETICAL CROOKED RIDGE RIVER

Topics of dispute and questions posed by Lucchitta and Holm (2019)	Interpretation of Lucchitta and Holm (2019)	Interpretations of Hereford et al. (2016) and this paper
Were the exotic clasts in the HCRR gravel derived from SJVF sources by direct fluvial transport, or were they reworked locally from previous piedmont deposits?	"HCCR was a river of regional importance that was headed in the San Juan volcanic field of SW Colorado" (p. 543); "…no piedmont that contained material derived from the San Juan Mountains is exposed or known in the region of interest" (p. 537).	A newly dated <9 Ma remnant deposit on Black Mesa, potentially correlative with the Bidahochi Formation, was part of a "piedmont source" of reworked clasts and SJVF sanidine. Bidahochi deposits near Ganado also contain abundant SJVF sanidine.
Was HCRR a river of regional significance, or was it merely a local stream?	HCRR "probably came into existence when these mountains were formed, and thus was of Miocene or Oligocene age" (p. 534); HCRR was " the principal stream…headed in the San Juan Mountains…that existed … perhaps as early as Oligocene time, until it was captured by the San Juan River, maybe ca. 2 Ma" (p. 533).	Fossil, sedimentological, and geochemical evidence indicates CRPR was in a low-energy channel system. Carbonate geochemistry shows sediment transport was not by waters of a high-elevation snowmelt river. Piracy of HCRR headwaters by the San Juan River ca. 2 Ma is rejected because it would require erosion rates of >700 m/m.y., many times the observed San Juan River incision rates at Bluff over the past 1.2 m.y. (125 m/m.y.).
Was the HCRR paleovalley large or small?	"The river flowed in a wide and deep valley…" (p. 543); "…10–15 km wide, in open reaches" (p. 539).	CRPR gradient (0.007) was comparable to that of Moenkopi Wash. Paleovalley width was 5–6 km on White Mesa and ~2.5 km at The Gap, a geomorphic remnant of the paleovalley. Elsewhere, its apparent width is enlarged due to subsequent erosion.
Is the age of HCRR Oligocene to early Miocene, or <2 Ma?	HCCR came into being in Miocene and possibly Oligocene time, which is when the very high San Juan Mountains were formed (p. 533); "…[there is a] very low probability given by the four [<2 Ma] grains actually measured from the White Mesa alluvium" (p. 540).	WMA is <2 Ma based on 42 new detrital sanidine dates. Minimum age is constrained by the ca. 1.1 Ma Red Lake tuff (this paper), inset 200 m below the WMA paleovalley.
Which alluvium best represents the alluvial history of the region, that of HCCR, or the WMA?	"The alluvium in the White Mesa region was deposited chiefly by local tributaries to Crooked Ridge river. The course of Crooked Ridge river can be traced through White Mesa on the basis of exotic clasts, which are not present in the alluvium of the tributaries" (p. 543).	The WMA is the same mapped unit as the alluvium on Crooked Ridge; both postdate 2 Ma and have similar detrital sanidine age distributions. Two of the White Mesa alluvium paleochannels carried exotic clasts; some did not, reflecting their local provenance. No physical or age basis requires separation of WMA from the alluvium on Crooked Ridge.
Did the HCRR cross the Kaibab uplift and, if so, when?	"HCRR joined the ancestral Colorado River and the ancestral Little Colorado River somewhere east of the Kaibab Plateau. From there, the combined rivers flowed across the upwarp in a valley located at or near the present eastern Grand Canyon. The subsequent course probably was toward the northwest, but the exact location is not known at the present time" (p. 543).	The CRPR postdates cutting of the East Kaibab paleocanyon. The East Kaibab paleocanyon model (Karlstrom et al., 2014, 2017), based on thermochronologic evidence, is that an ancestral Little Colorado River system incised across the Kaibab uplift 25–15 Ma, but the ancestral Colorado and San Juan Rivers were not involved.

HCRR—hypothetical Crooked Ridge River of Lucchitta and Holm (2019); SJVF—San Juan volcanic field; WMA—White Mesa alluvium; CRPR—Crooked Ridge paleoriver (this paper).

Heizler_GES02319 1st pages / 12 of 17

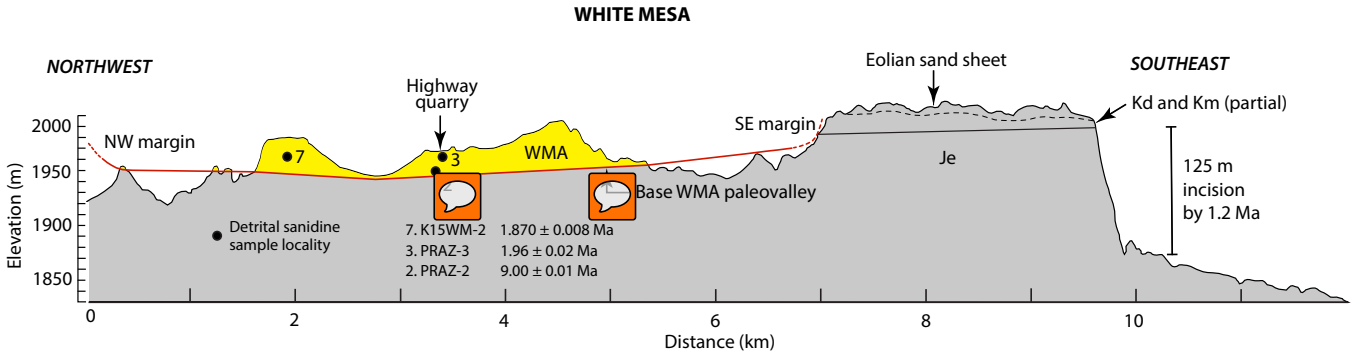

Figure 9. Transverse northwest-southeast cross-section of the White Mesa paleovalley on southern White Mesa, showing basal contact of White Mesa alluvium (WMA) on bedrock and stratigraphic position and sample number of dated detrital sanidines (from GPS-based field geologic mapping; Hereford et al., 2016, their figure 5). The White Mesa alluvium paleovalley profile lacks evidence of inset relations with older deposits, consistent with surface topography. Incision of the 125 m subvertical southeastern face of White Mesa was accomplished in <0.8 m.y. following deposition of White Mesa alluvium. Bedrock units: Je—Entrada Sandstone (Jurassic); Kd—Dakota Sandstone (Cretaceous); Km—Mancos Shale (Cretaceous).

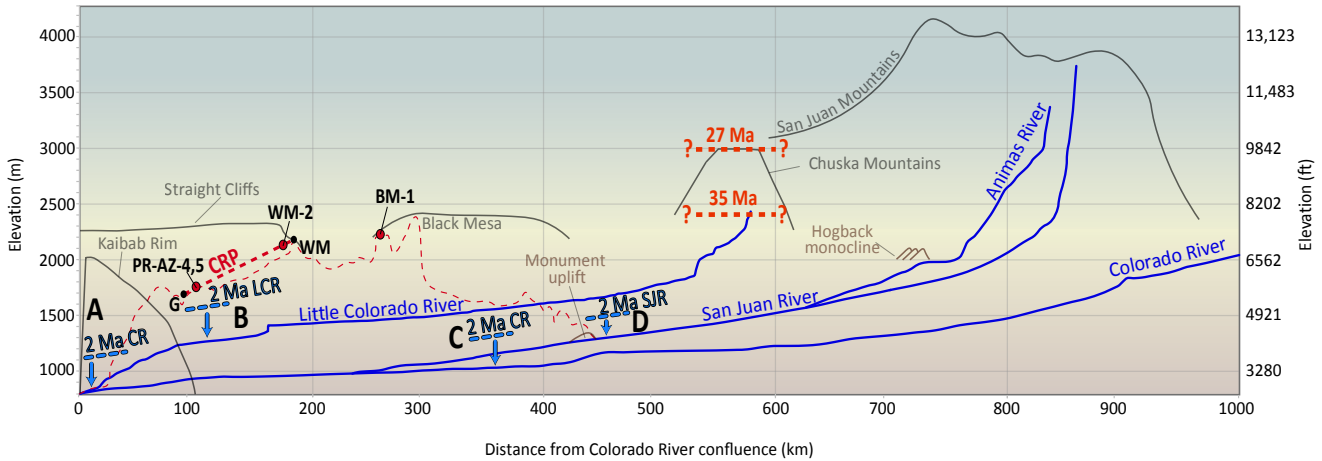

Figure 10. (A) Gradient of the hypothetical Crooked Ridge River relative to the Colorado, Little Colorado, and San Juan Rivers. Fine red dashed line is the modern topographic profile of the proposed path of Crooked Ridge River (Fig. 1) by Lucchitta et al. (2013); note the deep erosion required since ca. 2 Ma near the San Juan River. Heavy red dashed line labeled "CRP" shows the average 7 m/km gradient of the Crooked Ridge paleoriver between The Gap (G) and White Mesa (WM). Red dots show sample locations (see Fig. 1 and Table 1); Black Mesa sample (BM-1) is substantially below the projection of the Crooked Ridge paleoriver. The approximate 35 Ma and 27 Ma sub–Chuska Sandstone and top–Chuska Sandstone surfaces are shown as orange dashed lines. The late Oligocene San Juan Mountains profile (gray) is depicted as originally grading to the top of the Chuska Sandstone (Cather et al., 2008). Incision constraints A–D (see locations in Fig. 1) show inferred 2 Ma river levels assuming steady incision: A—Grand Canyon (Colorado River; CR) rates are >142 to <166 m/m.y. based on <172 m/1.21 m.y. from Unkar terraces (Karlstrom, 2019) and 445 m/2.68 m.y. from Butte fault speleothem (Crow et al., 2014); B—Little Colorado River (LCR) incision rates are 193 m/m.y. (172 m/0.89 m.y.) from the Black Point basalt (Karlstrom et al., 2017); C—Colorado River (CR) rates at Bullfrog Marina are 130 m/m.y. (195 m/1.5 m.y.; Darling et al., 2012); D—San Juan River (SJR) incision rates at Bluff, Utah, are 125 m/m.y. (151 m/1.2 m.y.) as updated from Wolkowinsky and Granger (2004) and maximum depositional age from detrital sanidine sample SJR-2 (see Table 1).

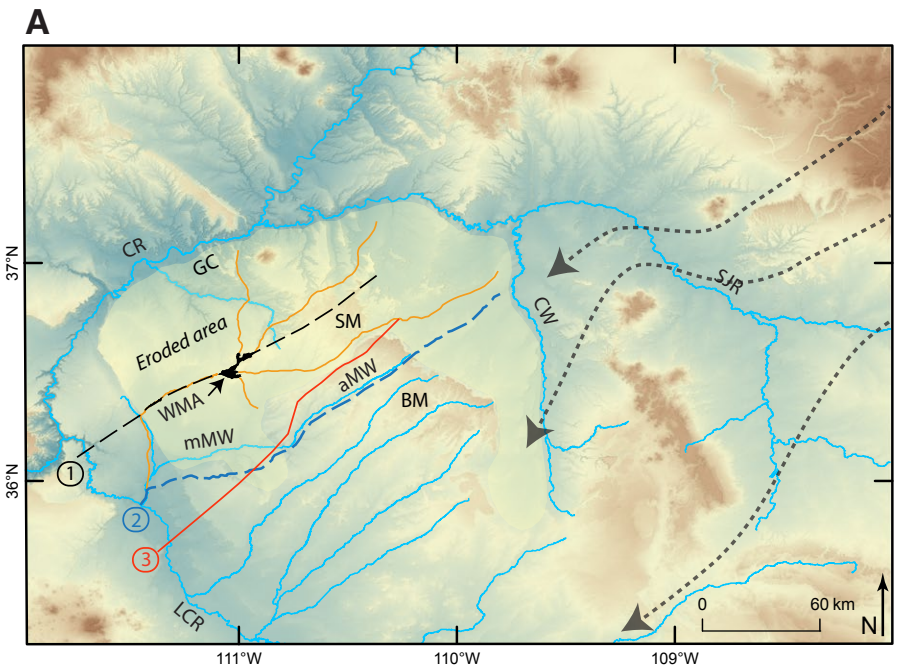

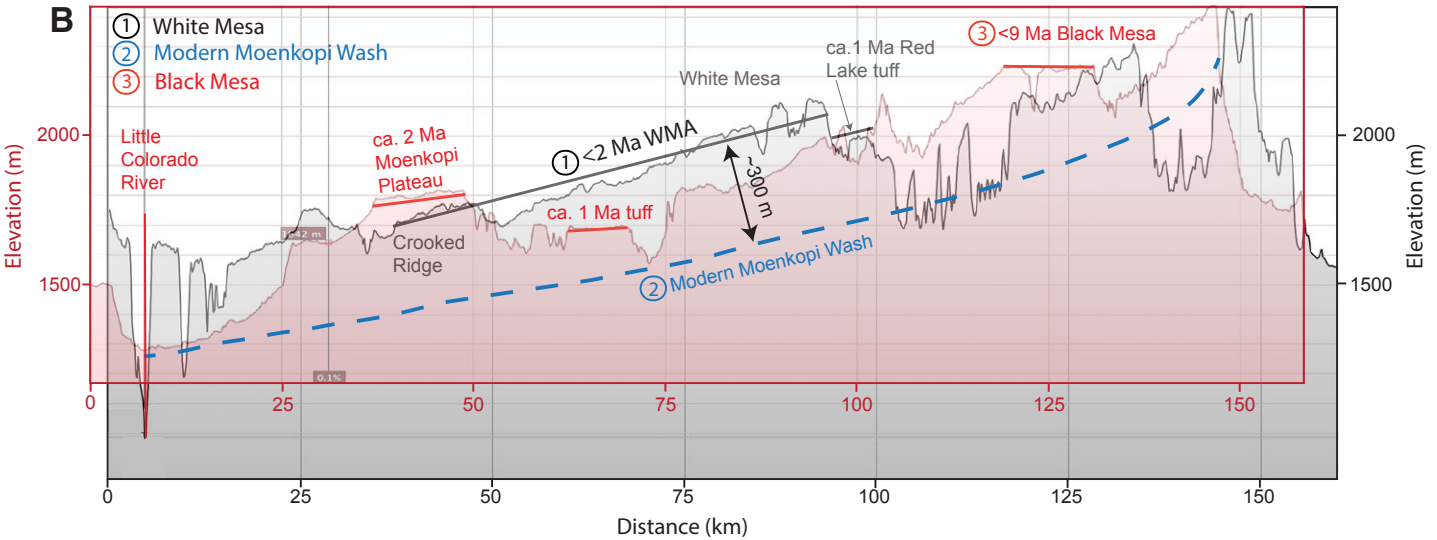

Figure 11. (A) Map summarizing an alternative interpretation to explain the <2 Ma age of the White Mesa alluvium, the abundant San Juan Mountains–derived detritus, and the geomorphic context of the Crooked Ridge paleoriver. Black Mesa (BM) retreated westward from Chinle Wash (CW) as indicated by numerous beheaded drainages on Black Mesa and Skeleton Mesa (SM), and southeastward from the rim of ancestral Glen Canyon (GC) of the Colorado River (CR). White Mesa alluvium (WMA) paleochannels (orange) and ancestral Moenkopi Wash (aMW) are from Hereford et al. (2016). Numbered lines are profiles (shown in B) along: (1) the Crooked Ridge paleoriver and White Mesa alluvium (black), (2) present Moenkopi Wash (blue), and (3) Black Mesa slope (red). Gray dotted arrows show possible Bidahochi-age alluvial pathways for detrital sanidine from the San Juan volcanic field. LCR—Little Colorado River; SJR—San Juan River. (B) Stacked profiles (see A for locations) showing the variably eroded White Mesa (gray, in background) and Black Mesa (transparent red) slopes compared to modern Moenkopi Wash (blue dashed line). The gradients of <1.9 Ma White Mesa alluvium (black line placed at base of deposits) and ca. 2 Ma Moenkopi Plateau (red line at base of deposits) are steeper (5–7 m/km) than the <9 Ma Black Mesa surface (approximately horizontal) due to base-level fall associated with integration of the Colorado River system after 5 Ma. The 2 Ma White Mesa alluvium paleoprofile is similar in gradient to the present Moenkopi Wash, both representing tributaries of the Little Colorado River. Tributary incision of Moenkopi Wash is ~150 m/m.y. over the past 2 m.y. Inset surface below White Mesa contains 1.07 Ma Red Lake tuff (sampled ~16 km south of White Mesa) that is similar in age and geomorphic position as the inset surface below Moenkopi Plateau containing both the Bishop and Glass Mountain Tuff (ca. 0.8–1.2 Ma) at Blue Canyon. Profiles were generated in Google Earth and equally scaled. The common point on the profiles is the junction with the Little Colorado River (LCR) placed at respective elevations.

Lipman, 1989). Figure 11B also shows that the gradient of modern Moenkopi Wash is similar to that of the Crooked Ridge paleoriver, and an approximate incision rate of [illegible]m/m.y. for Moenkopi Wash on Black Mesa in the past 2 m.y. is similar to values of the Crooked Ridge paleoriver (119–155 m/m.y.) based on the Blue Point tuff surface (Fig. 1; Karlstrom et al., 2017, their table 1).

Figure 12 serves to summarize different interpretations for how regional drainages evolved into the modern Grand Canyon landscape. As summarized above, the <2 Ma age of White Mesa alluvium (Fig. 6), the steep gradient and high landscape position relative to known depth of incision of the trunk rivers (Fig. 10), and lack of any major paleovalley preserved in the modern landscape (Fig. 12) are such that there is no physical evidence to support the hypothesis that the Crooked Ridge paleoriver was directly inherited from an older paleovalley system.

Thermochronologic data are beginning to provide constraints on past, now-eroded landscapes, and these data pose obstacles for the Lucchitta and Holm (2019) model. The segment of Grand Canyon across the Kaibab uplift, called the East Kaibab paleocanyon by Karlstrom et al. (2014), is proposed to have been carved to below the Kaibab Limestone between 25 and 15 Ma (Flowers et al., 2008; Lee et al., 2013). A <2 Ma Crooked Ridge paleoriver obviously could not have carved a 25–15 Ma East Kaibab paleocanyon but, Lucchitta and Holm (2019) argued, why couldn't a hypothesized combined Colorado–San Juan river have followed a similar path tens of millions of years earlier?

Thermochronology sample locations shown in Figure 1 show that rocks currently along the San Juan River across the Monument uplift (Fig. 12) and those in Marble Canyon along the Colorado River at Lees Ferry were still beneath 1–2 km of Mesozoic strata until after 6 Ma (Kelley et al., 2001; Flowers et al., 2008; Hoffman, 2009; Karlstrom et al., 2012b, 2014, 2017, 2020; Lee et al., 2013). Thus, any pre–6 Ma major ancestral river in these areas would have flowed at the level of the Mesozoic rocks above the Paria Plateau (at 2–2.5 km elevation; Fig. 12) and could not have been graded to the base of the East Kaibab paleocanyon, whose base was likely at 1.5-1.8 km elevation by 15 Ma (Karlstrom et al., 2017). Certainly, the elevations of Crooked Ridge, The Gap, and White Mesa are too low to be vestiges of this hypothetical river system. An alternative model is that the paleo–Little Colorado River carved the East Kaibab paleocanyon between 25 and 15 Ma (Karlstrom et al., 2014, 2017, 2020). Models for pre–6 Ma drainage patterns and future tests for the existence of ancestral Colorado and San Juan paleoriver-paleocanyon systems will benefit from additional thermochronologic data, estimates of isostatic responses to deep denudation (e.g., Lazear et al., 2013), and consideration of post–10 Ma differential uplift and tilting of the Colorado Plateau–Rocky Mountain region (Karlstrom et al., 2012b).

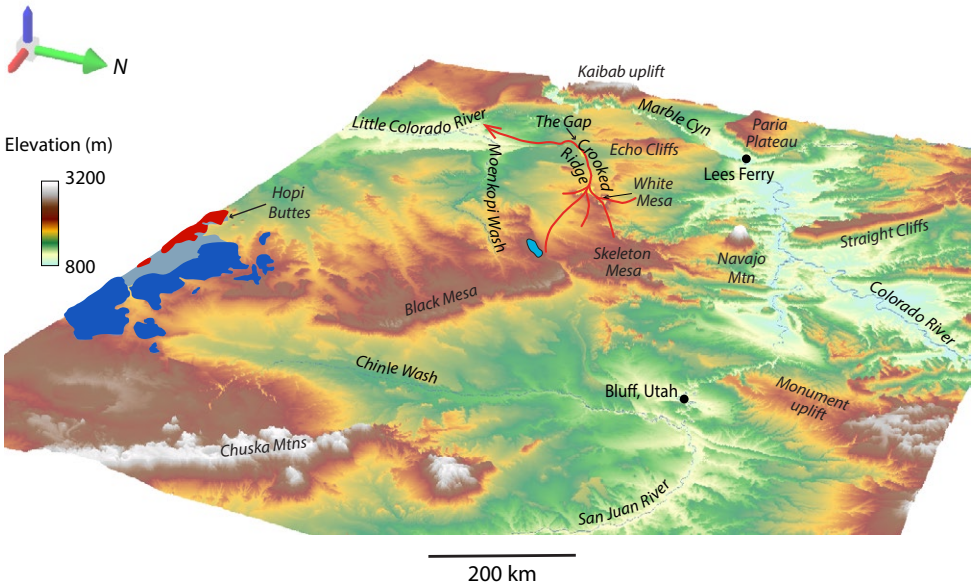

Figure 12. Oblique view, looking west, showing the inverted topography of <2 Ma Crooked Ridge paleoriver (red) relative to modern Colorado River and its tributaries. The Crooked Ridge paleoriver turned southwest near The Gap and likely joined the Little Colorado River near the present junction of Moenkopi Wash. Its headwaters tapped the fluvial Bidahochi Formation near Skeleton Mesa (now eroded) and Black Mesa (<9 Ma remnant deposits shown in cyan). Fluvial Bidahochi deposits are blue, fine-grained Bidahochi in light blue, and ca. 7 Ma Hopi Butte volcanic rocks are red. Perspective scene (5× vertical exaggeration) was created in ESRI ArcScene from a 10 m DEM.

CONCLUSIONS

Dating of ~1200 detrital sanidine grains with the $^{40}Ar/^{39}Ar$ dating from the White Mesa alluvium along with ~2300 grains from the Chuska Sandstone, Bidahochi Formation, and Colorado and San Juan River terraces provide resolution to a debate about the landscape evolution of the Four Corners region. These data show that the age of the White Mesa alluvium is <1.9 Ma. The regional inset relationships of the ca. 1.1 Ma Red Lake and Blue Canyon tuffs (Fig. 1) suggest this paleoriver aggraded and was abandoned between 1.9 and 1.1 Ma. San Juan volcanic field–sourced detrital sanidine grains are numerous in the White Mesa alluvium; however, this does not require a direct fluvial pathway from the San Juan Mountains at ca. 2 Ma because reworking of such grains from the Bidahochi Formation or age-equivalent deposits is likely.

The nature of hypothetical rivers that evolved into the modern drainage in the Four Corners region remains speculative because of the 1–2 km of material that has been eroded. We dispute the hypothetical Crooked Ridge River of Oligocene to early Pleistocene age as envisioned by Lucchitta and Holm (2019) for the following reasons: (1) all known deposits of the river are early Pleistocene; (2) there is no evidence that any paleovalley containing the hypothetical Crooked Ridge River was inherited directly from an older landscape; (3) the proposed piracy of the headwaters of the Crooked Ridge paleoriver by the San Juan paleoriver at 2 Ma would require a >700 m/m.y. incision rate near Four Corners, incompatible with measured incision rates of 140 m/m.y. over 1.2 m.y. at Bluff, Utah; and (4) thermochronologic data indicate 1–2 km of material has been eroded from the Monument upwarp and Marble Canyon in the past 5 m.y. (Karlstrom et al., 2014, 2017).

Instead, geochronological, geomorphic, and sedimentary evidence indicates that the Pleistocene Crooked Ridge paleoriver was a tributary to the Little Colorado River, analogous to modern Moenkopi Wash, that existed between 1.9 and 1.1 Ma and whose headwaters were pirated due to young, deep incision of Marble Canyon, Glen Canyon, and the San Juan River after 2 Ma.

ACKNOWLEDGEMENTS

We acknowledge U.S. National Science Foundation awards EAR-1348007 (to KEK) and EAR-1545986 (to LJC and KEK) for partial support. Field work by SMC was funded by the New Mexico Bureau of Geology and Mineral Resources. Detrital sanidine geochronology was funded with internal resources of the New Mexico Geochronology Research Laboratory. The manuscript benefited from insightful reviews by Steve Reynolds and Brian Jicha.

REFERENCES CITED

Babenroth, D.L., and Strahler, A.N., 1945, Geomorphology and structure of the East Kaibab monocline, Arizona and Utah: Geological Society of America Bulletin, v. 56, p. 107–150, https://doi.org/10.1130/0016-7606(1945)56[107:GASOTE]2.0.CO;2.

Cather, S.M., Peters, L., Dunbar, N.W., and McIntosh, W.C., 2003, Genetic stratigraphy, provenance, and new age constraints for the Chuska Sandstone (upper Eocene–lower Oligocene), New Mexico–Arizona, *in* Lucas, S.G., Semken, S.C., Berglof, W.R., and Ulmer-Scholle, D.S., eds., Geology of the Zuni Plateau: New Mexico Geological Society Field Conference Guidebook 54, p. 397–412.

Cather, S.M., Connell, S.D., Chamberlin, R.M., McIntosh, W.C., Jones, G.E., Potochnik, A.R., Lucas, S.G., and Johnson, P.S., 2008, The Chuska erg: Paleogeomorphic and paleoclimatic implications of an Oligocene sand sea on the Colorado Plateau: Geological Society of America Bulletin, v. 120, p. 13–33, https://doi.org/10.1130/B26081.1.

Cooley, M.E., and Davidson, E.S., 1963, The Mogollon Highlands—Their influence on Mesozoic and Cenozoic erosion and sedimentation: Arizona Geological Society Digest, v. 6, p. 7–35.

Cooley, M.E., Harshbarger, J.W., Akers, J.P., and Hardt, W.F., 1969, Regional hydrogeology of the Navajo and Hopi Indian reservations, Arizona, New Mexico, and Utah: U.S. Geological Survey Professional Paper 521-A, 61 p., https://doi.org/10.3133/pp521A.

Copeland, P., 2020, On the use of geochronology of detrital grains in determining the time of deposition of clastic sedimentary strata: Basin Research, https://doi.org/10.1111/bre.12441 (in press).

Coutts, D.S., Matthews, W.A., and Hubbard, S.M., 2019, Assessment of the widely used methods to derive depositional ages from detrital zircon populations: Geoscience Frontiers, v. 10, p. 1421–1435, https://doi.org/10.1016/j.gsf.2018.11.002.

Crow, R., Karlstrom, K., Darling, A., Crossey, L., Polyak, V., Granger, D., Asmerom, Y., and Schmandt, B., 2014, Steady incision of Grand Canyon at the million year timeframe: A case for mantle-driven differential uplift: Earth and Planetary Science Letters, v. 397, p. 159–173, https://doi.org/10.1016/j.epsl.2014.04.020.

Dallegge, T.A., Ort, M.H., and McIntosh, W.C., 2003, Mio-Pliocene chronostratigraphy, basin morphology and paleodrainage relations derived from the Bidahochi Formation, Hopi and Navajo Nations, northeastern Arizona: Mountain Geologist, v. 40, p. 55–82.

Darling, A.L., Karlstrom, K.E., Granger, D.E., Aslan, A., Kirby, E., Ouimet, W.B., Lazear, G.D., Coblentz, D.D., and Cole, R.D., 2012, New incision rates along the Colorado River system based on cosmogenic burial dating of terraces: Implications for regional controls on differential incision: Geosphere, v. 8, p. 1020–1041, https://doi.org/10.1130/GES00724.1.

Dickinson, W.R., 2013, Rejection of the lake spillover model for initial incision of the Grand Canyon, and discussion of alternatives: Geosphere, v. 9, p. 1–20, https://doi.org/10.1130/GES00839.1.

Dickinson, W.R., Cather, S.M., and Gehrels, G.E., 2010, Detrital zircon evidence for derivation of arkosic sand in the eolian Narbona Pass Member of the Eocene–Oligocene Chuska Sandstone from Precambrian basement rocks in central Arizona, *in* Fassett, J.E., Zeigler, K.E., and Lueth, V.W., eds., Geology of the Four Corners Country: New Mexico Geological Society Field Conference Guidebook 61, p. 125–134.

Flowers, R.M., Wernicke, B.P., and Farley, K.A., 2008, Unroofing, incision, and uplift history of the southwestern Colorado Plateau from apatite (U-Th)/He thermochronometry: Geological Society of America Bulletin, v. 120, p. 571–587, https://doi.org/10.1130/B26231.1.

Gehrels, G., 2014, Detrital zircon U-Pb geochronology applied to tectonics: Annual Review of Earth and Planetary Sciences, v. 42, p. 127–149, https://doi.org/10.1146/annurev-earth-050212-124012.

Henry, C.D., and John, D.A., 2013, Magmatism, ash-flow tuffs, and calderas of the ignimbrite flareup in the western Nevada volcanic field, Great Basin, USA: Geosphere, v. 9, p. 951–1008, https://doi.org/10.1130/GES00867.1.

Hereford, R., Beard, L.S., Dickinson, W.R., Karlstrom, K.E., Heizler, M.T., Crossey, L.J., Amoroso, L., House, P.K., and Pecha, M., 2016, Reevaluation of the Crooked Ridge river—Early Pleistocene (ca. 2 Ma) age and origin of the White Mesa alluvium, northeastern Arizona: Geosphere, v. 12, p. 768–789, https://doi.org/10.1130/GES01124.1.

Hoffman, M.D., 2009, Mio-Pliocene erosional exhumation of the central Colorado Plateau, eastern Utah: New insights from apatite (U-Th)/He thermochronometry [M.S. thesis]: Lawrence, University of Kansas, 176 p.

Hunt, C.B., 1969, Geologic history of the Colorado River, *in* Rabbitt, M.C., et al., The Colorado River Region and John Wesley Powell: U.S. Geological Survey Professional Paper 669, p. 59–130, https://doi.org/10.3133/pp669C.

Karlstrom, K.E., 2019, Fieldtrip booklet for GSA Grand Canyon Thompson Field Forum I, "Age and Carving of Grand Canyon: Towards a resolution of 150 years of debate" (September 14–21, 2019), https://orcid.org/0000-0003-2756-1724.

Karlstrom, K.E., Beard, L.S., House, K., Young, R.A., Aslan, A., Billingsley, G., and Pederson, J., 2012a, Introduction: CRevolution 2: Origin and Evolution of the Colorado River System II: Geosphere, v. 8, p. 1020–1041, https://doi.org/10.1130/GES00716.1.

Karlstrom, K.E., Coblentz, D., Dueker, K., Ouimet, W., Kirby, E., Van Wijk, J., Schmandt, B., Kelley, S., Lazear, G., Crossey, L.J., Crow, R., Aslan, A, Darling, A., Aster, R., MacCarthy, J., Hansen, S.M., Stachnik, J., Stockli, D.F., Garcia, R.V., Hoffman, M., McKeon, R., Feldman, J., Heizler, M., Donahue, M.S., and the CREST Working Group, 2012b, Mantle-driven dynamic uplift of the Rocky Mountains and Colorado Plateau and its surface response: Toward a unified hypothesis: Lithosphere, v. 4, p. 3–22, https://doi.org/10.1130/L150.1.

Karlstrom, K.E., Lee, J.P., Kelley, S.A., Crow, R.S., Crossey, L.J., Young, R.A., Lazear, G., Beard, L.S., Ricketts, J.W., Fox, M., and Shuster, D.L., 2014, Formation of the Grand Canyon 5 to 6 million years ago through integration of older paleocanyons: Nature Geoscience, v. 7, p. 239–244, https://doi.org/10.1038/ngeo2065.

Karlstrom, K.E., Crossey, L.J., Embid, E., Crow, R., Heizler, M., Hereford, R., Beard, L.S., Ricketts, J.W., Cather, S., and Kelley, S., 2017, Cenozoic incision history of the Little Colorado River: Its role in carving Grand Canyon and onset of rapid incision in the past ca. 2 Ma in the Colorado River system: Geosphere, v. 13, p. 49–81, https://doi.org/10.1130/GES01304.1.

Karlstrom, K.E., Jacobson, C.E., Sundell, K.E., Eyster, A., Blakey, R., Ingersoll, R.V., Mulder, J.A., Young, R.A., Beard, L.S., Holland, M.E., Shuster, D.L., Winn, C., and Crossey, L., 2020, Evaluating the Shinumo-Sespe drainage connection: Falsifying the "old" (70–17 Ma) Grand Canyon models for Colorado Plateau drainage evolution: Geosphere, https://doi.org/10.1130/GES02265.1 (in press).

Kelley, S.A., Chapin, C.E., and Karlstrom, K.E., 2001, Laramide cooling histories of the Grand Canyon, Arizona, and the Front Range, Colorado, determined from apatite fission-track

thermochronology, *in* Young, R.A., and Spamer, E.E., eds., Colorado River: Origin and Evolution: Grand Canyon Association Monograph 12, p. 37–42.

Kruskal, J.B., 1964, Nonmetric multidimensional scaling: A numerical method: Psychometrika, v. 29, p. 115–129, https://doi.org/10.1007/BF02289694.

Kuiper, K.F., Deino, A., Hilgen, F.J., Krijgsman, W., Renne, P.R., and Wijbrans, J.R., 2008, Synchronizing the rock clocks of Earth history: Science, v. 320, p. 500–504, https://doi.org/10.1126/science.1154339.

Lazear, G., Karlstrom, K.E., Aslan, A., and Kelley, S., 2013, Denudation and flexural isostatic response of the Colorado Plateau and southern Rocky Mountain region since 10 Ma: Geosphere, v. 9, p. 792–814, https://doi.org/10.1130/GEO00836.1.

Lee, J.P., Stockli, D.F., Kelley, S.A., Pederson, J.L., Karlstrom, K.E., and Ehlers, T.A., 2013, New thermochronometric constraints on the Tertiary landscape evolution of central and eastern Grand Canyon, Arizona: Geosphere, v. 9, p. 216–228, https://doi.org/10.1130/GES00842.1.

Lipman, P.W., 1989, Excursion 16B: Oligocene–Miocene San Juan volcanic field, *in* Chapin, C.E., and Zidek, J., eds., Field Excursions to Volcanic Terranes in the Western United States, Volume 1: Southern Rocky Mountains Region: New Mexico Bureau of Mines and Mineral Resources Memoir 46, p. 303–380.

Lipman, P.W., and McIntosh, W.C., 2008, Eruptive and noneruptive calderas, northeastern San Juan Mountains, Colorado: Where did the ignimbrites come from? Geological Society of America Bulletin, v. 120, p. 771–795, https://doi.org/10.1130/B26330.1.

Lipman, P.W., Zimmerer, M.J., and McIntosh, W.C., 2015, An ignimbrite caldera from the bottom up: Exhumed floor and fill of the resurgent Bonanza caldera, Southern Rocky Mountain volcanic field, Colorado: Geosphere, v. 11, p. 1902–1947, https://doi.org/10.1130/GES01184.1.

Love, D.W., 1989, Bidahochi Formation: An interpretive summary, *in* Anderson, O.J., Lucas, S.G., Love, D.W., and Cather, S.M., eds., Southeastern Colorado Plateau: New Mexico Geological Society Field Conference Guidebook 40, p. 273–280.

Lucchitta, I., and Holm, R., 2019, Re-evaluation of exotic gravel and inverted topography at Crooked Ridge, northern Arizona: Relicts of an ancient river of regional extent: Geosphere, v. 16, p. 533–545, https://doi.org/10.1130/GES02166.1.

Lucchitta, I., Holm, R.F., and Lucchitta, B.K., 2011, A Miocene River in northern Arizona and its implications for the Colorado River and Grand Canyon: GSA Today, v. 21, no. 10, p. 4–10, https://doi.org/10.1130/G119A.1.

Lucchitta, I., Holm, R.F., and Lucchitta, B.K., 2013, Implications of the Miocene(?) Crooked Ridge River of northern Arizona for the evolution of the Colorado River and Grand Canyon: Geosphere, v. 9, p. 1417–1433, https://doi.org/10.1130/GES00861.1.

Mahon, K.I., 1996, The new "York" regression: Application of an improved statistical method to geochemistry: International Geology Review, v. 38, p. 293–303, https://doi.org/10.1080/00206819709465336.

Massey, F.J., Jr., 1951, The Kolmogorov-Smirnov test for goodness of fit: Journal of the American Statistical Association, v. 46, p. 68–78, https://doi.org/10.1080/01621459.1951.10500769.

McIntosh, W.C., Chapin, C.E., Ratté, J.C., and Sutter, J.F., 1992, Time-stratigraphic framework for the Eocene-Oligocene Mogollon-Datil volcanic field, southwest New Mexico: Geological Society of America Bulletin, v. 104, p. 851–871, https://doi.org/10.1130/0016-7606(1992)104<0851:TSFFTE>2.3.CO;2.

McKee, E.D., Wilson, R.F., Breed, W.J., and Breed, C.S., eds., 1967, Evolution of the Colorado River in Arizona: An Hypothesis Developed at the Symposium on Cenozoic Geology of the Colorado Plateau in Arizona, August 1964: Museum of Northern Arizona Bulletin 44, 67 p.

Min, K., Mundil, R., Renne, P.R., and Ludwig, K.R., 2000, A test for systematic errors in $^{40}Ar/^{39}Ar$ geochronology through comparison with U/Pb analysis of a 1.1-Ga rhyolite: Geochimica et Cosmochimica Acta, v. 64, p. 73–98, https://doi.org/10.1016/S0016-7037(99)00204-5.

Repenning, C.A., Lance, J.F., and Irwin, J.H., 1958, Tertiary stratigraphy of the Navajo Country, *in* Anderson, R.Y., and Harshbarger, J.W., eds., Guidebook of the Black Mesa Basin, northeastern Arizona: New Mexico Geological Society Field Conference Guidebook 9, p. 123–129.

Saylor, J.E., and Sundell, K.E., 2016, Quantifying comparison of large detrital geochronology data sets: Geosphere, v. 12, p. 203–220, https://doi.org/10.1130/GES01237.1.

Saylor, J.E., Jordan, J.C., Sundell, K.E., Wang, X., Wang, S., and Deng, T., 2018, Topographic growth of the Jishi Shan and its impact on basin and hydrology evolution, NE Tibetan Plateau: Basin Research, v. 30, p. 544–563, https://doi.org/10.1111/bre.12264.

Schaen, A.J., Jicha, B.R., Hodges, K.V., Vermeesch, P., Stelten, M.E., Mercer, C.M., Phillips, D., Rivera, T.A., Jourdan, F., Matchan, E.L., Hemming, S.R., Morgan, L.E., Kelley, S.P., Cassata, W.S., Heizler, M.T., Vasconcelos, P.M., Benowitz, J.A., Koppers, A.A.P., Mark, D.F., Niespolo, E.M., Sprain, C.J., Hames, W.E., Kuiper, K.F., Turrin, B.D., Renne, P.R., Ross, J., Nomade, S., Guillou, H., Webb, L.E., Cohen, B.A., Calvert, A.T., Joyce, N., Ganderød, M., Wijbrans, J., Ishizuka, O., He, H., Ramirez, A., Pfänder, J.A., Lopez-Martínez, M., Qiu, H., and Singer, B.S., 2020, Interpreting and reporting $^{40}Ar/^{39}Ar$ geochronologic data: Geological Society of America Bulletin, https://doi.org/10.1130/B35560.1 (in press).

Strahler, A.N., 1948, Geomorphology and structure of the West Kaibab fault zone and Kaibab Plateau, Arizona: Geological Society of America Bulletin, v. 59, p. 513–540, https://doi.org/10.1130/0016-7606(1948)59[513:GASOTW]2.0.CO;2.

Vermeesch, P., 2013, Multi-sample comparison of detrital age distributions: Chemical Geology, v. 341, p. 140–146, https://doi.org/10.1016/j.chemgeo.2013.01.010.

Wolkowinsky, A.J., and Granger, D.E., 2004, Early Pleistocene incision of the San Juan River, Utah, dated with ^{26}Al and ^{10}Be: Geology, v. 32, p. 749–752, https://doi.org/10.1130/G20541.1.